Valorizing Steelworks Gases by Coupling Novel Methane and Methanol Synthesis Reactors with an Economic Hybrid Model Predictive Controller

Alexander Hauser [1,*], Philipp Wolf-Zoellner [2], Stéphane Haag [3], Stefano Dettori [4], Xiaoliang Tang [3], Moein Mighani [3], Ismael Matino [4], Claudio Mocci [4], Valentina Colla [4], Sebastian Kolb [1], Michael Bampaou [5], Kyriakos Panopoulos [5], Nina Kieberger [6], Katharina Rechberger [7] and Juergen Karl [1]

[1] Chair of Energy Process Engineering, Friedrich-Alexander-Universität Erlangen-Nürnberg, Fürther Straße 244f, 90429 Nürnberg, Germany; sebastian.kolb@fau.de (S.K.); juergen.karl@fau.de (J.K.)
[2] Chair of Process Technology and Industrial Environmental Protection, Montanuniversität Leoben, Franz-Josef-Str. 18, 8700 Leoben, Austria; philipp.wolf-zoellner@unileoben.ac.at
[3] AIR LIQUIDE Forschung und Entwicklung GmbH, Gwinnerstrasse 27-33, 60388 Frankfurt am Main, Germany; stephane.haag@airliquide.com (S.H.); xiaoliang.tang@airliquide.com (X.T.); moein.mighani@airliquide.com (M.M.)
[4] TeCIP Institute, School of Advanced Studies Sant'Anna, Via Moruzzi 1, 56124 Pisa, Italy; s.dettori@santannapisa.it (S.D.); i.matino@santannapisa.it (I.M.); claudio.mocci@santannapisa.it (C.M.); valentina.colla@santannapisa.it (V.C.)
[5] Chemical Process & Energy Resources Institute, Centre for Research and Technology Hellas, 6th km Charilaou-Thermi Road, 57001 Thessaloniki, Greece; bampaou@certh.gr (M.B.); panopoulos@certh.gr (K.P.)
[6] Voestalpine Stahl GmbH, voestalpine-Straße 3, 4020 Linz, Austria; nina.kieberger@voestalpine.com
[7] K1-MET GmbH, Stahlstraße 14, 4020 Linz, Austria; katharina.rechberger@k1-met.com
[*] Correspondence: alexander.hauser@fau.de

Abstract: To achieve the greenhouse gas reduction targets formulated in the European Green Deal, energy- and resource-intensive industries such as the steel industry will have to adapt or convert their production. In the long term, new technologies are promising. However, carbon capture storage and utilization solutions could be considered as short-term retrofitting solutions for existing steelworks. In this context, this paper presents a first experimental demonstration of an approach to the utilization of process off-gases generated in a steelworks by producing methane and methanol in hydrogen-intensified syntheses. Specifically, the integration of two methane synthesis reactors and one methanol synthesis reactor into a steel plant is experimentally simulated. An innovative monitoring and control tool, namely, a dispatch controller, simulates the process off-gas production using a digital twin of the steel plant and optimizes its distribution to existing and new consumers. The operating states/modes of the three reactors resulting from the optimization problem to be solved by the dispatch controller are distributed in real time via an online OPC UA connection to the corresponding experimental plants or their operators and applied there in a decentralized manner. The live coupling test showed that operating values for the different systems can be distributed in parallel from the dispatch controller to the test rigs via the established communication structure without loss. The calculation of a suitable control strategy is performed with a time resolution of one minute, taking into account the three reactors and the relevant steelworks components. Two of each of the methane/methanol synthesis reactors were operated error-free at one time for 10 and 7 h, respectively, with datasets provided by the dispatch controller. All three reactor systems were able to react quickly and stably to dynamic changes in the load or feed gas composition. Consistently high conversions and yields were achieved with low by-product formation.

Keywords: steelworks gas valorization; methane synthesis; methanol synthesis; predictive control; carbon capture and usage; hydrogen enrichment

1. Introduction

The European process industry is committed to align its objectives with the expectation of the European Union (EU), which plans a sustainable growth through the European Green Deal [1] and the "Fit for 55" legislative package [2] to achieve the ambitious goal of the reduction in greenhouse gases (GHG) by 55% compared to 1990 and pave the way for carbon neutrality in 2050. Consequently, energy- and resource-intensive industries such as steelworks are transforming their production routes to lower their GHG emissions.

The steel sector, which is responsible for about 6% of the total EU emissions [3], designed the Clean Steel Partnership (CSP) to tackle the twofold challenge of countering climate change and supporting sustainable growth in the EU [4] and is investing in the development of technologies to progressively reduce CO_2 emissions.

The work reported in the present paper fits this context by addressing the valorization of process off-gases (POGs) generated in integrated steelworks and providing valuable products, i.e., methane and methanol.

POGs derive from different steps of steel production from virgin raw materials: coke oven gas (COG) is generated by the ovens producing carbon coke, blast furnace gas (BFG) derives from materials melting to generate pig iron, and basic oxygen furnace gas (BOFG) is output by the converter transforming pig iron into steel through carbon removal. The POG composition depends strongly on the feedstock used and the process conditions of the individual sub-processes. Table 1 reports the main average features of the POGs relevant for this paper's case study.

Table 1. Main process off-gas features (averages) [5].

Compound/Feature	Unit	COG [b,c]	BFG [c]	BOFG [c]
N_2	mol.%	2.9	48.3	27.6
CO_2	mol.%	1.2	23.1	20.0
CO	mol.%	5.8	24.9	51.8
H_2	mol.%	65.7 [c]	3.7	0.6
CH_4	mol.%	21.8	traces	-
C_nH_m	mol.%	2.5	traces	-
O_2	mol.%	0.1	traces	traces
NCV [a]	kWh/Nm^3	5.9	1.0	2.4
Other features	-	Significant content of minor compounds (i.e., potential catalyst poisons)	Continuously produced	Discontinuously produced
Main users (in decreasing order)	-	Power plant, hot rolling mill, mixing and enrichment station, coke plant area, plate annealing, blast furnace area	Mixing and enrichment station [d], blast furnace area	Mixing and enrichment station [d]

[a] CH_4 NCV = 10.5 kWh/Nm^3. [b] COG composition measurement takes place after a gas cleaning unit (i.e., filter or desulphurization). [c] POG compositions are in good agreement with the values given in the BAT document [6] and in further literature papers [7–9]. [d] Mixed enriched gas is mainly used in power plant, coke ovens, and blast furnaces.

BFG and BOFG are rich in CO_x, while COG holds the highest amount of H_2. Usually, POGs are used internally, and their fate is mainly linked to their net calorific value (NCV): COG is highly used in the steelworks' power plant (PP) as it is, while other POGs are often mixed and/or enriched with natural gas (NG) to increase their NCV.

POG production and usage is often discontinuous and/or not synchronized. Thus, two limiting conditions can arise: a lack of gas, compensated by NG purchase, and excess gas, compensated by flaring, with the consequent release of CO_2 and energy waste. Internal electricity production is not always the best solution to exploit POGs if one considers CO_2 emissions: With respect to NG (or methane), BFG and BOFG hold significantly lower

NCVs and show potentially negative effects on CO_2 emissions. For this reason, Zhang et al. suggest reducing BFG consumption in the power plant [10].

Considering this background, two kinds of solutions can be followed to improve the valorization of POGs:

- Optimal management avoiding limiting conditions;
- Alternative POG routes exploiting carbon capture storage and usage (CCS and CCU) solutions.

Both approaches are relevant in the transition period towards C-lean production processes, such as the ones using hydrogen for the direct reduction of iron ore [11–13], as during the transition POGs will still be produced.

On POG network management, relevant work was carried out by Porzio et al. [14,15] concerning POG distribution and by Maddaloni et al. [16] on gas network layout optimization. More recently, an online tool for the optimal real-time management of POGs was proposed in [17,18], which also exploits machine learning (ML) [19–21].

CCS and CCU are considered in the smart carbon usage (SCU) pathway provided by the CSP [22]. CCS solutions (e.g., standard and innovative chemical absorption) can lead to significant decreases in global warming potential (between 48 and 76%) [23], especially if applied to BFG [24,25]. Important achievements can also be obtained through CCU technologies for the production of chemicals or fuels from POGs due to their similarity to syngas. For instance, the Fischer–Tropsch process can exploit POGs as feedstock [26] and ammonia can also be produced with them [27].

The present paper addresses methane and methanol production in an innovative way, as suggested in [28], by establishing a synergy between different sectors (i.e., steel, chemical, energetic, and automation) to maximize the advantages conveyed by CCS and CCU. In particular, experimental campaigns are presented in which the potential integration of synthesis reactors into steelworks is experimentally simulated. For this purpose, a previously developed control tool (dispatch controller) calculates the optimized operating control trends for three synthesis reactors (methane/methanol) based on hydrogen-enriched POGs from the steel industry. These data are made available to the decentralized reactors in real time via an online connection and the specified load and concentration gradients are applied live.
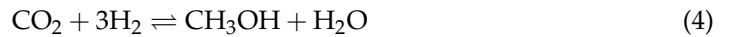
The paper is organized as follows: the state-of-the-art method of methane and methanol production from steelworks POGs is depicted in Section 2, together with a brief overview of the exploited control methodology. Section 3 presents the reactors and controller exploited in the experiments. Section 4 summarizes the main results, while Section 5 provides some concluding remarks and hints for future work.

2. State-of-the-Art Analysis

The idea of methanol production in steelworks is not new: the first investigations date back to the 1980s [29,30]. However, only in the last decade, the technology became mature enough to be considered as a valid CCU solution [31–34]. Nevertheless, the approaches are not optimized for today's challenges related to smaller capacities, integration into other processes (e.g., steelworks,) and fluctuating operation (e.g., related to POG availability and/or H_2 availability from renewables). Recently, these challenges have increasingly become the focus of research [7,35–39]. In addition, the techno-economic evaluation of these processes is of great interest [40–42].

Conversely, methane production from CO_2-rich gases is quite recent. The main studies on methanation from steelworks POGs refer to use of COG [43,44], which, however, decreases the availability of the most suitable POG for internal heating and power production. Furthermore, only preliminary investigations can be found on the use of BFG and BOFG [45,46], including some works of the authors that were the basis of the investigation presented in this work [47,48].

Methane and methanol synthesis involve the following hydrogenation reactions ((1) and (2) for methane and (3) and (4) for methanol) and the water gas shift reaction (5):

$$CO + 3H_2 \rightleftharpoons CH_4 + H_2O \tag{1}$$

$$CO_2 + 4H_2 \rightleftharpoons CH_4 + 2H_2O \tag{2}$$

$$CO + 2H_2 \rightleftharpoons CH_3OH \tag{3}$$

$$CO_2 + 3H_2 \rightleftharpoons CH_3OH + H_2O \tag{4}$$

$$CO_2 + H_2 \rightleftharpoons CO + H_2O \tag{5}$$

Suitable ratios among reagents are needed as well as ad hoc catalysts to allow high reagent conversions and the related significant product yields. In particular, the stoichiometric number (*SN*), defined as follows, is commonly used to express the ratios among the reagents:

$$SN_{CH_4} = \frac{[H_2]}{3[CO] + 4[CO_2]} \in \begin{bmatrix} 1 & 1.1 \end{bmatrix} \tag{6}$$

$$SN_{CH_3OH} = \frac{[H_2] - [CO_2]}{[CO] + [CO_2]} \in \begin{bmatrix} 1.5 & 2.1 \end{bmatrix} \tag{7}$$

The required SN ranges and the POG compositions (see Table 1) highlight that BFG and BOFG must be enriched in hydrogen before the syntheses. The amount of required hydrogen is significant, and green hydrogen production (e.g., through polymer electrolyte membrane (PEM) electrolysis powered by green electricity) is fundamental to achieve GHG emission reduction [49–51].

To sum up, valorizing POGs through methane and methanol synthesis requires addressing a series of issues. Some of them are specific to steelworks, such as the management of synthesis processes with uncommon feedstocks and in uncommon fluctuating operations, hydrogen production through green processes, and POG distribution towards new users. In addition, standard POG management and usage cannot be neglected.

Therefore, reactors for methanation and methanol production can be included in integrated steelworks only by coupling them with an ad hoc developed control system that considers the different constraints related to all the involved sub-processes and accounts for the volatility of energy commodity markets.

An evolution of model predictive control (MPC) was adopted here (see Section 3.4). MPC is a control approach developed in industrial contexts and deepened by numerous academic studies that have defined its main characteristics and amplified its effectiveness [52].

The previously mentioned coupling was tested and is reported in the present paper targeting the following objectives:

- The synchronization and control of different processes belonging to the steelmaking (i.e., internal gas users), energetic (i.e., power plant), chemical (i.e., synthesis reactors), and electrochemical (i.e., H_2 production process) domains;
- The suitable distribution of POGs between standard and novel users;
- POG mixing (both pure and mixed POGs can be fed to the reactors) and enrichment with hydrogen for optimal usage in synthesis reactors;
- The correct operation of the communication structure for the transmission of the control values to the real synthesis plants;
- The smooth operation of synthesis reactors with dynamics in feed gas composition and load;
- Optimized methane and methanol production, usage, and sale.

3. Materials and Methods

Two concepts of methanation reactors and a novel pilot plant for methanol production were exploited and coupled to an ad hoc developed supervision and control system. Their behavior under dynamic conditions was tested by reproducing the flows and compositions of POG feedstock to the synthesis reactors and related hydrogen enrichment as indicated by the control system by mixing bottled dry gases. For this reason, no additional purification processes of the synthetic POGs were required; these treatment steps would have been necessary in the case of real POGs, as described in [50].

These concepts are described in the following subchapters.

3.1. Lab-Scale Methanation Unit at Friedrich-Alexander-Universität Erlangen-Nürnberg (FAU)

A lab-scale methanation test rig (FAU_CH4_TR) placed at FAU in Nürnberg, Germany was used for the experiments. Figure 1 shows its simplified flowchart [48]. The test rig was designed for a maximum syngas power (P_{syn}) of 5 kW (related to the NCV of the reactants) and can be operated at pressures up to 5 bar. It comprised two methanation stages that were operated in series to obtain a higher carbon conversion. Between these stages, a condenser separated the water formed during the reaction, and the gas was pre-heated before entering the second reactor. Gas sampling points after the first and second reactor stage enabled the analysis of intermediate and product gas using an AO2000 analyzer (ABB Automation GmbH, Mannheim, Germany).
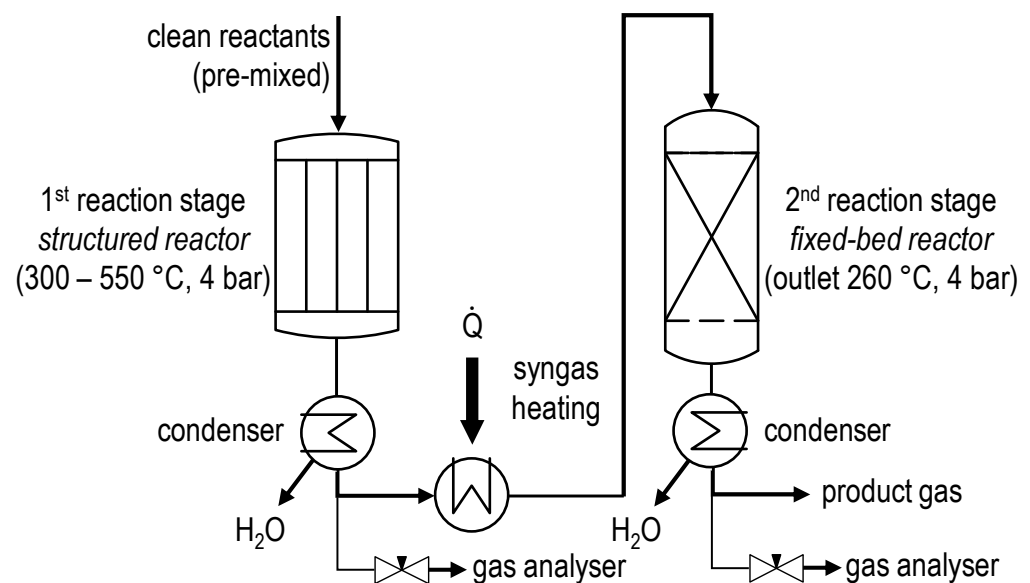

Figure 1. Simplified flowchart of FAU_CH4_TR [48].

The first reactor stage was designed as a heat-pipe cooled, structured fixed-bed reactor. The design conditions are presented in [53], and its main aim was the advanced temperature control of the highly exothermic methanation reaction.

The structured fixed-bed reactor (see Figure 2) had a total of nine reaction channels with diameters of 8 mm each, which were incorporated in a steel reactor body and contained semi-commercial catalyst pellets (Ni/Al_2O_3). To remove the reaction heat from the main reaction zone and the reactor, the reactor had 16 drillings in which 16 heat pipes fit exactly. Furthermore, drillings for internal gas preheating, reactant distribution, gas redirection, and product gas collection were incorporated in the reactor body. Figure 2 shows an exemplary gas pathway. To cool the heat pipes, defined volume flows of compressed air could be applied to their condenser zones. Heating cartridges allowed reactor preheating at start-up and trace heating during experiments. Several thermocouples recorded the temperature conditions of the reactor; in particular, three of them measured the temperatures at different axial positions at the wall of a reaction channel. A thermowell was inserted into the

central reaction channel, where a thermocouple could be automatically moved along the vertical direction by means of a linear motor. Due to the slow travel speed, quasi-stationary temperature profiles could be recorded along the reactor axis.
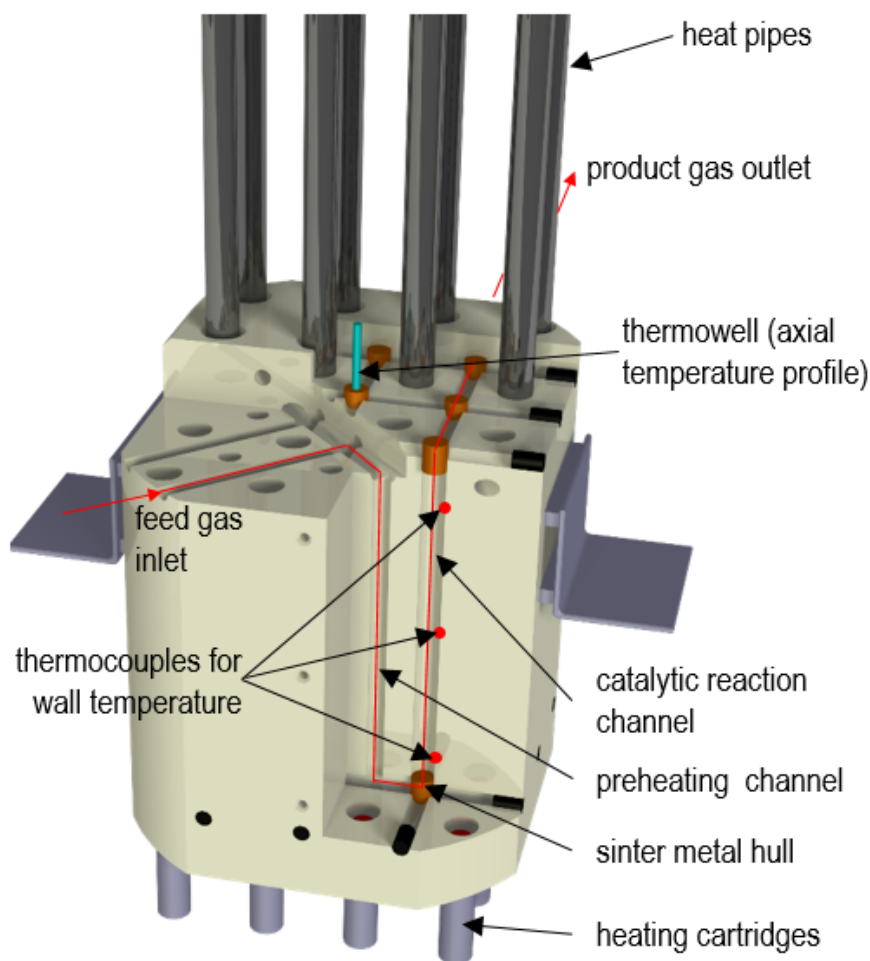

Figure 2. Cutaway scheme of the FAU structured reactor and exemplary gas pathway (reprint from [53] with permission from Elsevier).

The second reactor stage was designed as a classic fixed bed with an inner diameter of 27.6 mm. It could be cooled by compressed air through a double jacket and heated electrically. This reactor was oversized and was used to achieve full conversion.

3.2. Lab-Scale Methanation Unit at Montanuniversität Leoben (MUL)

The second methanation test rig (MUL_CH4_TR) was located at MUL in Leoben, Austria [47,54] and consisted of three cylindrical reactors (DN80, height 300 mm) operated in series (for a simplified flowchart see Figure 3). Each reactor was either filled with commercial Ni-based bulk catalyst or with wash-coated ceramic honeycomb monoliths [54]. In both cases, a volume of 0.25 L per reactor was covered with catalyst, and the remaining part was filled with an inert material (stoneware balls). The dimensions and design specifications of the reactors met the following operating parameters:

- Flow rate range: 0.3–3 Nm^3/h ($\approx$5–50 NL/min);
- Gas hourly space velocity (*GHSV*) range: 1200–12,000 h^{-1};
- Pressure rating: up to 20 bar;
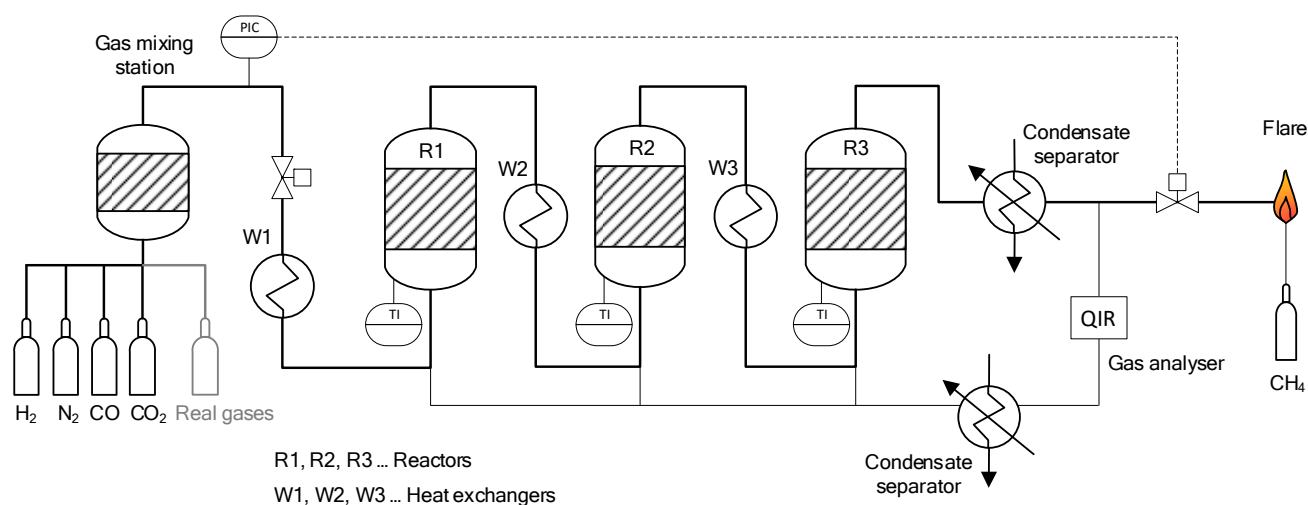- Maximum reactor temperature: 700 °C.

Figure 3. Simplified flowchart of MUL_CH4_TR [47].

Furthermore, four gas sampling stations were installed, allowing the composition analysis of both inlet and produced stream after each reactor stage. A URAS 26 infrared photometer was used for measuring CO, CO_2, and CH_4, while a CALDOS 27 thermal conductivity analyzer measured H_2 (both from ABB AG, Wiener Neudorf, Austria). The final product gas stream was cooled and guided through a condensate separator to extract any H_2O formed during synthesis. The product gases were combusted in a flare connected to the aspiration system. The reactor temperatures were measured with multi-thermocouples, providing an axial profile of the temperature distribution inside each reactor. In addition, the MUL_CH4_TR included heat exchangers up- and downstream of the reactors, a water dosing pump at the reactant gas side, a cooling unit, and a water separator as well as heating sleeves coating the outside of each reactor.

3.3. Pilot Plant for Methanol Synthesis at Air Liquide Forschung und Entwicklung (ALFE)

The novel pilot plant for methanol synthesis (ALFE_CH3OH_PLP) was located at Air Liquide Forschung und Entwicklung (ALFE) in Frankfurt am Main, Germany. It was designed to optimize the transformation of the CO_x contained in POGs into methanol and was successfully started in 2020.

The configuration of the new multi-stage setup allowed the adaption of the reaction section as desired to optimize the conversions of gases with different compositions (max. of four stages with inter-stage condensation). Therefore, this plant could deal with unconventional gas compositions, such as those of POGs, under once-through conditions or with low recycling at very fast response times regarding changes in loads and/or in gas compositions.

The key features of this pilot plant can be described as follows:

- Several reactor stages;
- Various possible flow schemes;
- Heat transfer to steam system;
- Temperature profile measurement in the different process stages through multi-point thermocouples;
- Throughput:
  - Feed gas up to 35 Nm^3/h;
  - Raw methanol product up to 20 kg/h.

Figure 4 presents pictures of the outdoor and indoor parts of ALFE_CH3OH_PLP.

(**a**)

(**b**)

Figure 4. (**a**) Outdoor and (**b**) indoor sections of ALFE_CH3OH_PLP.

For the test campaign, four stages were filled with a commercial methanol catalyst. The reaction section consisted of several stages set up for the optimal conversions of CO, CO_2, and H_2 (X_{CO}, X_{CO2}, and X_{H2}, respectively) combined with fast adaption to changing conditions. Between each stage there was the possibility to remove the produced raw methanol. The collected methanol/water mixture was then analyzed to determine the amounts of by-products. The new unit allowed high overall methanol production and extended the lifetime of the catalyst. The operation in the ALFE_CH3OH_PLP using four stages filled with catalyst under once-through operation can be described as follows:

- Fresh feed gas was fed to stage 1 of the reaction section;
- Unconverted gases from stage 1 were fed to stage 2;
- Unconverted gases from stage 2 were fed to stage 3;
- Unconverted gases from stage 3 were fed to stage 4;
- Raw methanol product was removed after each stage and analyzed accordingly;
- By-product amounts were evaluated in the raw methanol removed between the stages;
- The final raw methanol product gathered all the contributions coming from each stage.

One major advantage to using a once-through multi-stage concept for fluctuating loads and fluctuating off-gas compositions is that the time of response is significantly lower than for a setup with high recycling. Therefore, only a few minutes were necessary without recycling to have the desired feed composition and load at the reactor (or stage) inlet in the methanol plant, which was not the case when traditional recycling was used. Typically, by using classical recycling, a few hours would be required to provide the desired conditions at the reactor inlet in terms of feed composition and load.

Moreover, the multi-stage concept with once-through operation is much more flexible regarding the amount of inerts in the feed (nitrogen and/or methane). These inerts can rapidly lead to accumulation at the reactor inlet when recycling. The multi-stage concept can be operated regardless of the composition of the feed and can still produce a raw methanol that is able to be treated in a classical distillation section. This concept fits perfectly for a coupling with an advanced control system, as the desired conditions at the reactor/stage inlet are fixed quickly. This allows the adaption of all the parameters to optimize the operating conditions in a very short time in order to maximize methanol production and to lower by-product formation to ensure a proper distillation.

The online analytical concept is based on process gas chromatography. The system was developed and implemented for the analysis of syngas composition and methanol as well as some main by-products in a single gas phase with a broad concentration range and a detection limit of 0.01 mol.% or better.

In particular, hot gas streams from reactor outlets, unconverted gases, methanol, water, and some oxygenates under high pressure and temperature can be online analyzed in the gas phase using a dedicated online sample conditioning and analysis system. Moreover, a

gas stream dilution system can be applied for hot gas streams once the chromatography signal is saturated. Additionally, a continuous evaporation mixture system is integrated as a validation system to monitor the conditioning and analysis system with methanol and water vapor mixture during operation in a certain time interval. The online analytical system, including a heated conditioning system, a four-channel micro-GC system, and a continuous evaporation mixture system is shown in Figure 5.

Figure 5. Online conditioning and analysis system of ALFE_CH3OH_PLP.

The short response time of the online analyzer enables the real-time optimization of process variables and the adjustment of feedstock composition to control the side reactions and achieve the desired product yield.

3.4. Dispatch Controller at ICT-COISP Center of TeCIP Institute of Scuola Superiore Sant'Anna

The supervision and control system exploited in the test campaign, from now on named the dispatch controller (DC), was developed at Scuola Superiore Sant'Anna (SSSA) in Pisa, Italy to investigate the integration of the synthesis reactors into steelworks and to online optimize POG distribution to the synthesis reactors while considering all the issues related to POG management and the interactions between gas networks and gas consumers. A schematic overview of the concept of the POG-based methane and methanol production and control system is depicted in Figure 6, where the coupling between the POG networks, synthesis reactors, power plant, hydrogen production system, and DC is highlighted.

To optimize the production of methane and methanol from POGs, several factors must be considered. First, POG production, standard usage, and gasholder dynamics must be taken into account. POG excess is stored in gasholders, which hold minimum and maximum level limits and, in general, show quite fast dynamics, as they tend to fill and empty in about 30–60 min, depending on the steelworks size. POG availability is varied by leading synthesis reactors to work under variable load conditions, which are characterized by highly non-linear dynamics that make their control challenging.

POG-based methane and methanol production requires gas enrichment by large amounts of hydrogen, the production of which is very energy-intensive. To ensure economic and environmental sustainability, green electricity sources must be exploited for hydrogen production, especially in the hours when energy is cheaper [49,50].
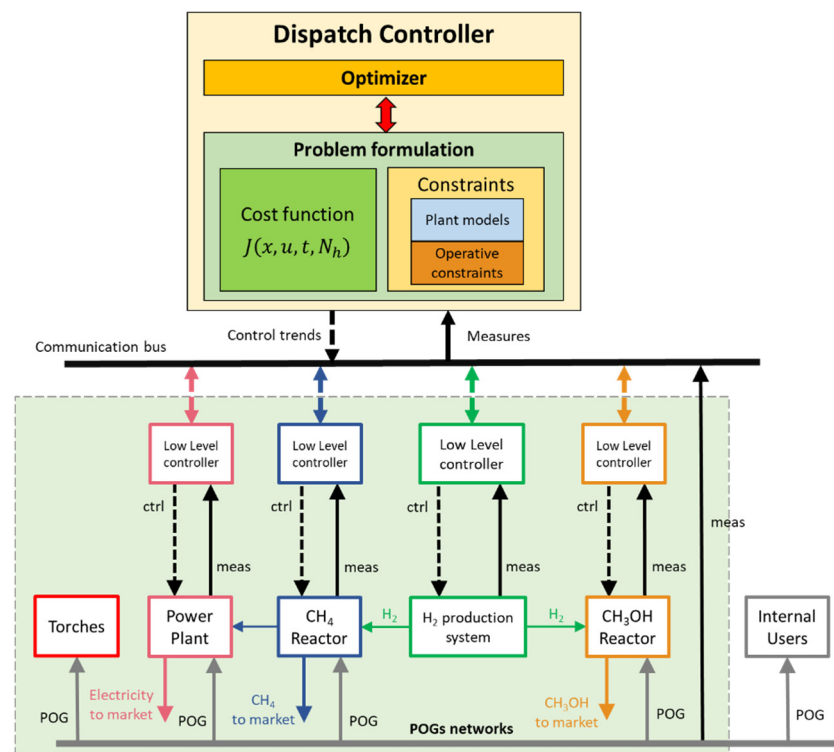
Figure 6. Conceptual coupling between DC and POG-based methane and methanol production units.

The mentioned plants and processes can be mathematically modelled through input/output correlations that often require the use of discrete control variables. For instance, synthesis reactors can operate in different discrete modes (i.e., OFF, standby, only BFG, only BOFG, and mixed gas), power plant groups can be switched on/off according to the amount of power to be produced, and the hydrogen production system (e.g., PEM electrolyzers) is composed of different stacks that can be switched on/off, depending on the required amount of hydrogen. Furthermore, the DC must be able to calculate an appropriate control action in real time to deal with variable POG availability.

The DC was developed through a methodology based on the economic hybrid model predictive control (EHMPC) [55], which maximizes revenues and minimizes environmental impact while complying with the constraints of each plant and process. Details on the design strategy, mathematical implementation and preliminary results were presented in the paper of some of the authors [56], where the main characteristics were reported. The optimization problem is formulated as a mixed integer linear programming (MILP) for a receding horizon, where the cost function to be maximized is calculated as follows:

$$J(x, u, t, N_h) = \sum_{k=t}^{t+N_h} \alpha^k \Big(R_{ES}(k) + R_{MEOH}(k) + R_{CH4}(k) + R_{CO_2}(k) - C_{PEM}(k) - C_T(k) - C_{fOPEX}(k) \Big) \tag{8}$$

where x and u are, respectively, the state of the system and the manipulated variables, t is the current time, N_h the prediction horizon, k is the time along the prediction horizon, R_{ES} is the revenue related to the electricity sold to the external grid, and R_{MEOH} and R_{CH4} are, respectively, the revenues related to the methanol and methane sold. C_{PEM} is the price of the green electricity consumed by the PEM electrolyzer system, C_T is the cost of wasting POG excess in the torches, and C_{fOPEX} are the fictitious operative costs that penalize the continuous switching of reactors and PEM stacks, the variation in gas volume flow at the reactor inlet, and the decreasing of gasholder levels below a security threshold. The economic costs related to the environmental impact of the CO_2 emissions in integrated steelworks typically depend on the amount of virgin coal-based raw materials exploited and on the purchased natural gas. For this reason and considering that the CO_2

emissions related to virgin coal-based raw materials are not affected by POG management, R_{CO_2} is calculated here as the revenue related to CO_2 cost savings due to internal methane production. At the present stage of the research, the economic costs do not take into account the eventual operative costs of methane and methanol clean-up equipment and treatments.

The constraints of the optimization problem mathematically describe the dynamics of each reactor, power plant group, PEM electrolyzer, and gasholder and the operative limits of each piece of equipment and unit. Each unit and piece of equipment was modelled by a linear state space model whose parameters were tuned using real data. The reactors' models were designed in MATLAB/Simulink (R2020b, MathWorks®, Natick, MA, USA) by implementing the physical/chemical equations of synthesis reactions and thermal transmission [57]; these equations were tuned using real data of the reactors and of preliminary experimental tests. Each synthesis reactor model did not take into account the clean-up stages and related operative costs.

Furthermore, the DC included a set of advanced models forecasting future POG excess (i.e., digital twins of steelworks units involved in POG production and storage) and the costs of energy media (electricity, methane, and methanol), both developed through ML techniques. The models forecasting POG excess were developed using real data of voestalpine steelworks located in Linz (Austria), which were used also in this work for simulating a possible real application of methane and methanol synthesis processes [58].

The DC calculated the control strategy for a time window of 2 h ahead with a control period of 1 min. Every control period, the controller linearized the reactor models around the last operative point, allowing the solution of a linear optimization problem within a fixed maximum time of 30 s.

3.5. Data Communication Infrastructure

Figure 7 shows the data communication infrastructure established for the live tests, which was required due to the different locations of the reactors and dispatch controller.
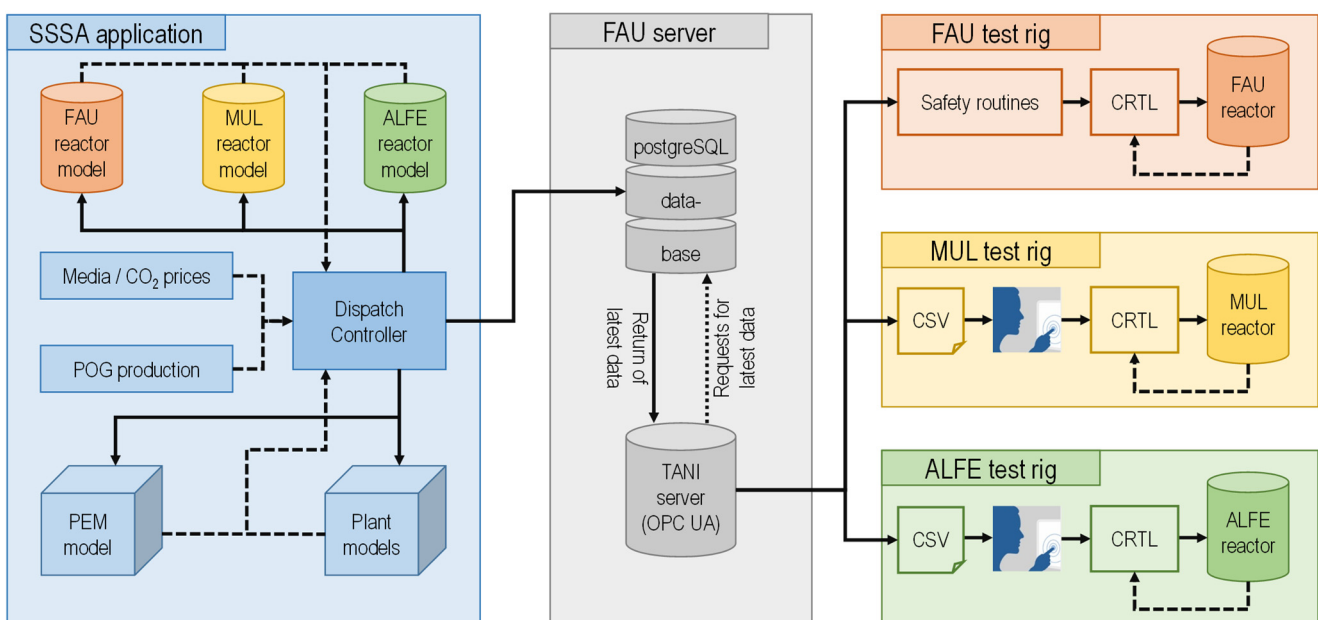
Figure 7. Data communication structure between DC and test rigs for online test campaign.

The DC is highlighted in blue on the left side with all related models and input parameters. This routine maximized the objective function (Equation (8)) by iterating the feedback generated from the individual models for the PEM electrolysis, the three synthesis reactors, as well as eleven further models mapping the various steelworks units. It performed calculations every minute and wrote the best solution for the following POG operating parameters into a PostgreSQL database (grey section, middle): total volumetric

flow rate, gas composition, pressure, and temperature. These data included the solution for the current timestamp and a look ahead for the upcoming two hours, which was available for FAU_CH4_TR (orange, top right), MUL_CH4_TR (yellow, middle right), and ALFE_CH3OH_PLP (green, bottom right) to be retrieved. Therefore, an open platform communications unified architecture (OPC UA) server was implemented, which sent queries to the database in selectable regular intervals and requested the last valid dataset. Three query routines were included, each of them requested the operating values for one test rig. Once the data exchange took place successfully, human operators checked the suggested parameters at MUL_CH4_TR and ALFE_CH3OH_PLP to ensure safe plant operations. For FAU_CH4_TR, automated safety routines took this task and checked, e.g., whether the stoichiometry (Equation (6)) and syngas power matched the reactor limits. Therefore, the datasets were handed over directly to the plant's programmable logic controller (PLC) via the OPC UA. When an incoming dataset did not meet the specifications, it was ignored, and the test rig was further operated with the last valid dataset.

With respect to the conceptual idea (described in Section 3.4), the DC interacted with digital twins of the integrated steelworks and the synthesis reactors in the live test campaign presented in this paper. For safety reasons, at the current stage of development, the coupling between the DC and reactors was simulated through the models without direct feedback of the real state of each piece of involved equipment. Since the DC delivered the control strategy to the synthesis reactors without receiving any direct feedback from the real plants, the overall system operated in an open loop.

4. Results and Discussion

Different scenarios were designed and then live tested where, generally, two reactors were operated in parallel. The following subchapters describe the experimental online coupling campaign and the main results.

4.1. Definition of Scenarios

To evaluate the validity of the approach to synthesize methane and methanol from POGs and the integration of this solution in integrated steelworks, two essential aspects need to be assessed: (i) the ability of the controller to calculate optimal control trends in real time and (ii) the ability of the synthesis reactors and test rigs to work, even under particularly variable dynamic conditions. To these aims, a set of scenarios was defined through a wide campaign of offline simulations in which the advanced models of the reactors and the digital twin of the considered integrated steelworks was used. In order to obtain indications suitable for both the laboratory setup and for the possible development of future industrial plants, the DC interacted with virtual reactors that were linearly scaled up with respect to the pilot/bench-scale ones. In more detail, the industrial scales of the reactors were evaluated to produce a methane amount sufficient to satisfy the steelworks' needs and a methanol amount sufficient for commercial purposes.

The first phase of the simulation campaign was devoted to a fine tuning of the controller and optimizer parameters to balance the aggressiveness of the control action on the plants and the computational time; some simulated control trends were reported in [56,59] where the results of a preliminary investigation on economic cost improvement were also presented. In [59], the authors reported a first attempt at sensitivity analysis, varying the price of renewable sources of electricity for producing green hydrogen, and an estimate of CO_2 emission reductions.

Different scenarios for the online test campaign were tested, among which the most significant ones are:

- Scenario 1 (SC1): two methane reactors (FAU_CH4_TR and MUL_CH4_TR) running in parallel in variable load conditions with strong disturbances in the BFG network, where several sequential BFG shortages are simulated;
- Scenario 2 (SC2): one methane (FAU_CH4_TR) and one methanol (ALFE_CH3OH_PLP) reactor running in parallel with variable operating conditions due to a BFG shortage.

This scenario is of particular interest, as it allows the simulation of a context in which it is possible to access the product market (i.e., methane, methanol, and possibly electricity) in which the flexibility and diversification of production could be an economically winning factor. In particular, considering the current variability in the prices of both electricity and products such as methane, it is considered fundamental to test the validity of the developed control approach.

To obtain sufficient variability in the control trends and to verify the behavior of the reactors at different operating points, each scenario was designed to simulate the operation of reactors characterized by different industrial scales and different disturbances in the POG networks. The main idea was testing the DC and the plants in extreme conditions characterized by fast dynamics in a wide range and variability in the inlet gas both in terms of flow rate and composition. This implies a different POG distribution to the plants and the possibility, for instance, of making the reactors work within the maximum operating points (by decreasing the industrial scale of the reactors, a greater relative availability of POGs was observed) or with greater variability within the operating ranges (with reactors characterized by larger industrial scales or the simulation of a temporary shortage of POGs). In order to better understand the nature of the simulated disturbances, the starting scenario data refer, in terms of POG production, to the data of the industrial partner of the project, which are related to a "constant and standard" steel production period. Regarding the internal POG consumption, on the other hand, we referred to an average consumption baseline within the integrated steelworks plant and some artificial disturbances simulated on top of them. Artificial additional disturbances had the purpose of testing the behavior of both control systems and reactors in extreme conditions.

Furthermore, all the scenarios were characterized by a set of constant boundary conditions:

- POGs distributed to the power plant and synthesis reactors;
- Produced methanol sold to external users;
- Produced methane distributed to external users and internal consumers based on the economic gain;
- A warmup phase followed by about 10–12 h of methane and/or methanol production;
- The methane reactors exploited BFG and BOFG with the constant stoichiometric number $SN_{CH_4} = 1.04$;
- The methanol reactor exploited BFG, BOFG, and COG with $SN_{CH_3OH} \in \begin{bmatrix} 1.5 & 2.1 \end{bmatrix}$;
- The price of electricity sold to the external grid was equal to EUR 80/MWh;
- The prices of methane and methanol sold to external users were equal to EUR 25/MWh and EUR 400/ton, respectively;
- The price of CO_2 emissions was equal to EUR 30/ton;
- The price of green electricity for the PEM electrolyzer was equal to EUR 5/MWh;
- The number of available PEM electrolyzer stacks was equal to 70, each characterized by a nominal power of 17.5 MW and a resulting hydrogen production of 340 kg/h at full capacity.

Exemplary results obtained in the two mentioned scenarios are depicted in Figures 8–13, which were calculated online during the live test campaign and exploited as control references for the involved reactors. In particular, Figure 8a depicts SC1 in terms of POG production in blue and internal consumption in orange (from top to bottom, respectively, BFG, BOFG, and COG). Figure 8b shows the POG distribution to the PP (blue) and reactors (orange), respectively, for BFG and BOFG, while the third diagram shows the methane produced and distributed to the PP (blue) and to external users (orange). Figure 9 depicts the bench-scale control action calculated by the DC for FAU_CH4_TR. In more detail, Figure 9a shows the POG volume flow and hydrogen mixture at the inlet of the reactor and its limits in the function of the modality (only BFG, only BOFG, or a mixture of both), while Figure 9b shows the control action in terms of inlet gas composition. Figure 10 depicts the same control action in the case of MUL_CH4_TR running in parallel.
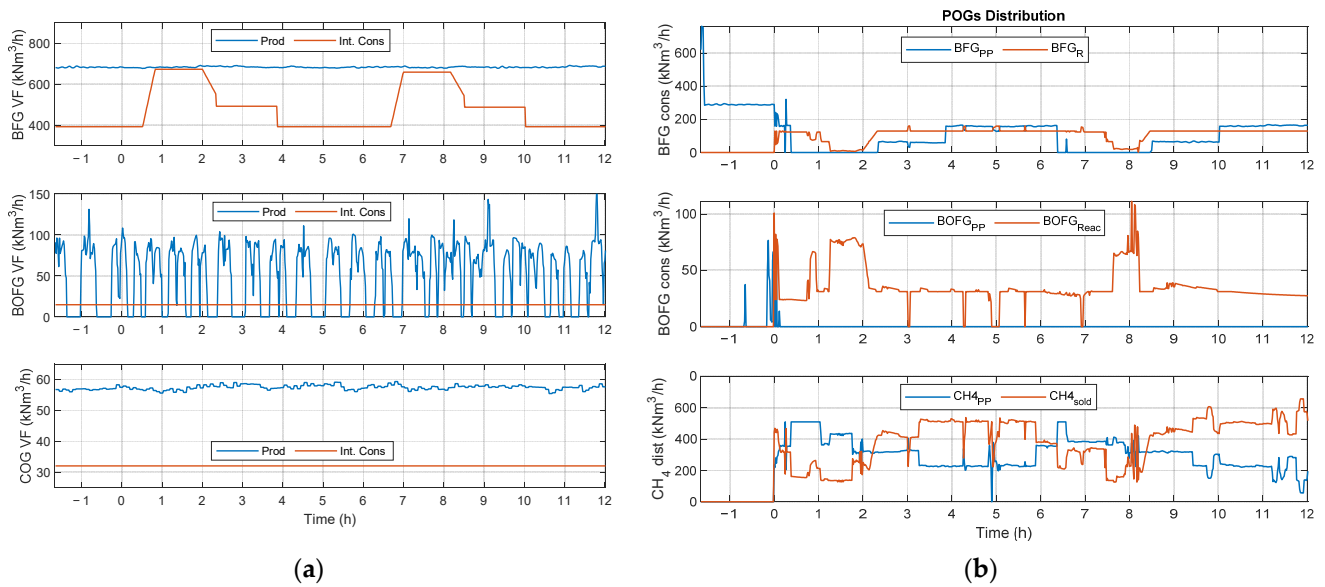
Figure 8. SC1. (**a**) POG production and consumption by internal users; (**b**) POG distribution to PP and methane reactors and methane consumption in PP and sent to market.
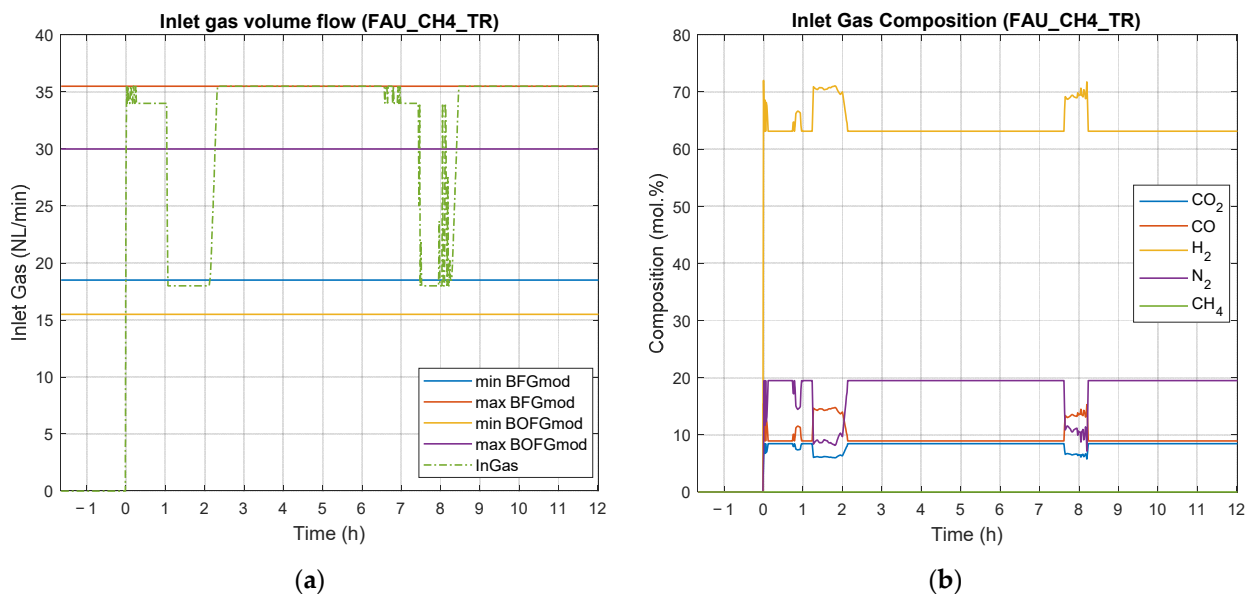

Figure 9. SC1. Control strategy for FAU_CH4_TR. (**a**) Inlet gas volume flow; (**b**) inlet gas composition.

The representation of Figure 11 reports the same information as Figure 8 but for SC2 and extended by the methanol sent to market (yellow) in Figure 11b. Figure 12 represents the control action calculated by the DC for FAU_CH4_TR in bench scale during SC2, while Figure 13 depicts the control action for the methanol plant ALFE_CH3OH_PLP running in parallel.

An in-depth analysis of the results of the scenarios revealed several interesting behaviors. They are described below together with some preliminary results regarding potential reductions of CO_2 emissions.

In SC1, the objective was to achieve a sufficient variability in load conditions. Figure 8a shows two sequential disturbances in BFG availability: two simulated shortages of BFG (between 0.5–2.5 h and between 6.5–8.5 h), during which the main POG in terms of quantity was less available for the methanation process. The BFG shortages drove reactors to work in several dynamic conditions and led the DC to calculate a control action that decreased the

BFG consumption in both the reactors and PP (see Figure 9b) with a consequent switching of FAU_CH4_TR to BOFG/mixed gas modalities with suitable hydrogen enrichment to reach the required SN_{CH4}. Concerning MUL_CH4_TR, it mainly ran through BOFG enriched with hydrogen with few switches to the BFG modality. The COG was exploited only in the PP, while the produced methane was distributed to the PP and market with a certain variability. Regarding the CO_2 reduction in the SC1 period, an approximate evaluation was conducted by starting from the rough estimate provided in [59]. The reduction in CO_2 in the SC1 period was about 1151 t, corresponding to a reduction of about 62% with respect to the CO_2 emissions that would have been obtained by feeding the same amount of POGs exploited in the synthesis reactors directly to a power plant. At the same time, the produced CH_4 usage in power plant in replacement of the POGs allowed the production of an amount of electrical energy 1.65 times higher.
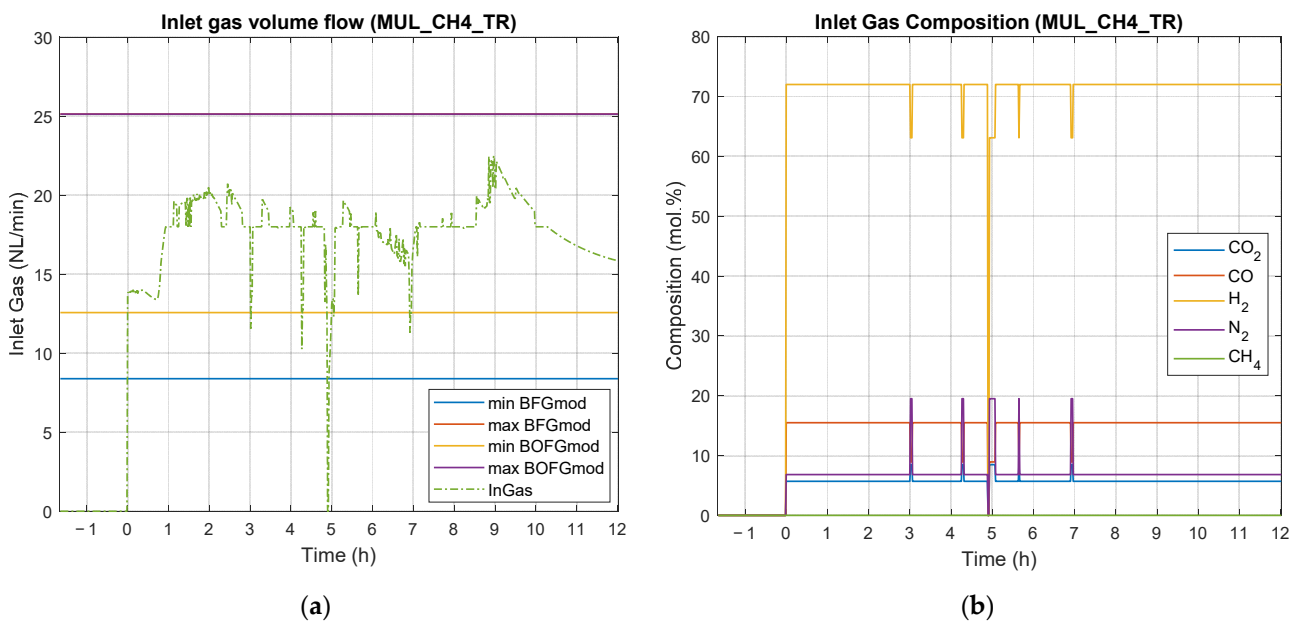

Figure 10. SC1. Control strategy for MUL_CH4_TR. (**a**) Inlet gas volume flow; (**b**) inlet gas composition.
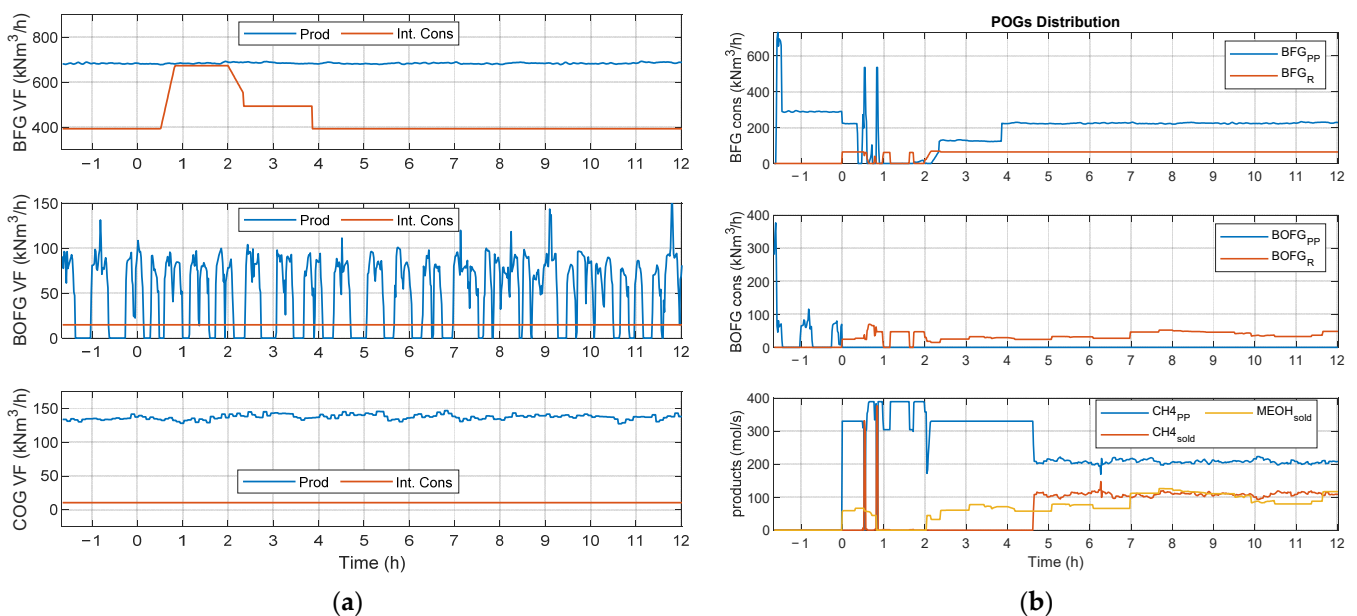

Figure 11. SC2. (**a**) POG production and consumption by internal users; (**b**) POG distribution to PP and methane reactors, methane consumption in PP and sent to market, and methanol sold.
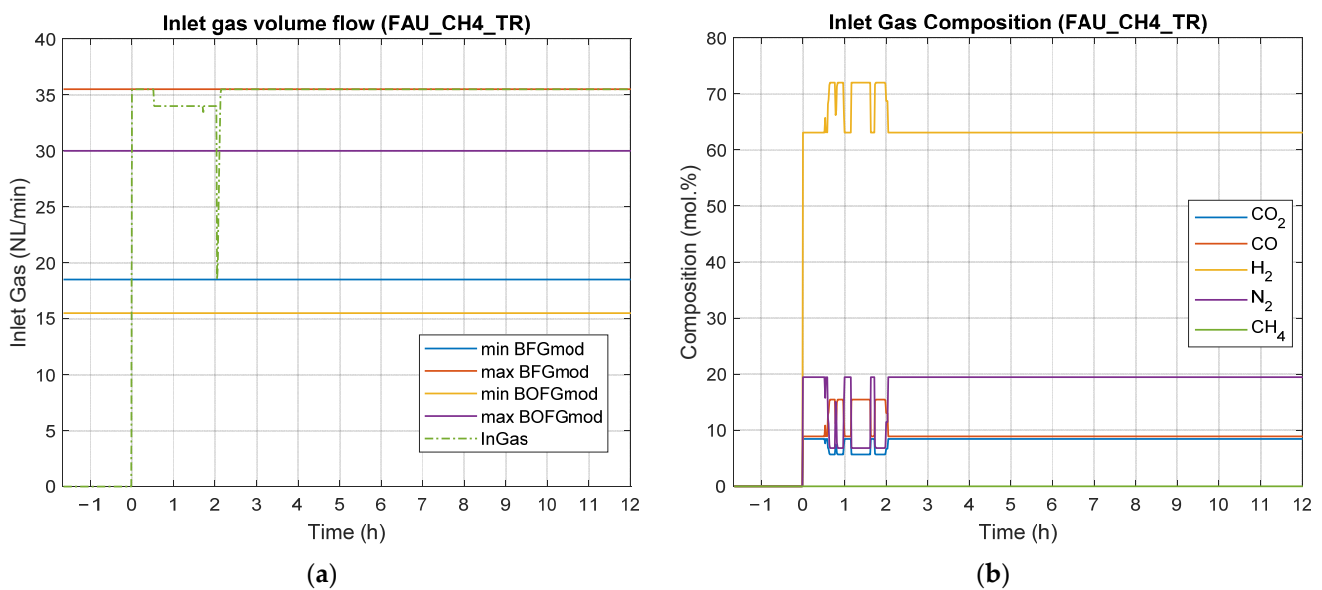
Figure 12. SC2. Control strategy for FAU_CH4_TR. (**a**) Inlet gas volume flow; (**b**) inlet gas composition.
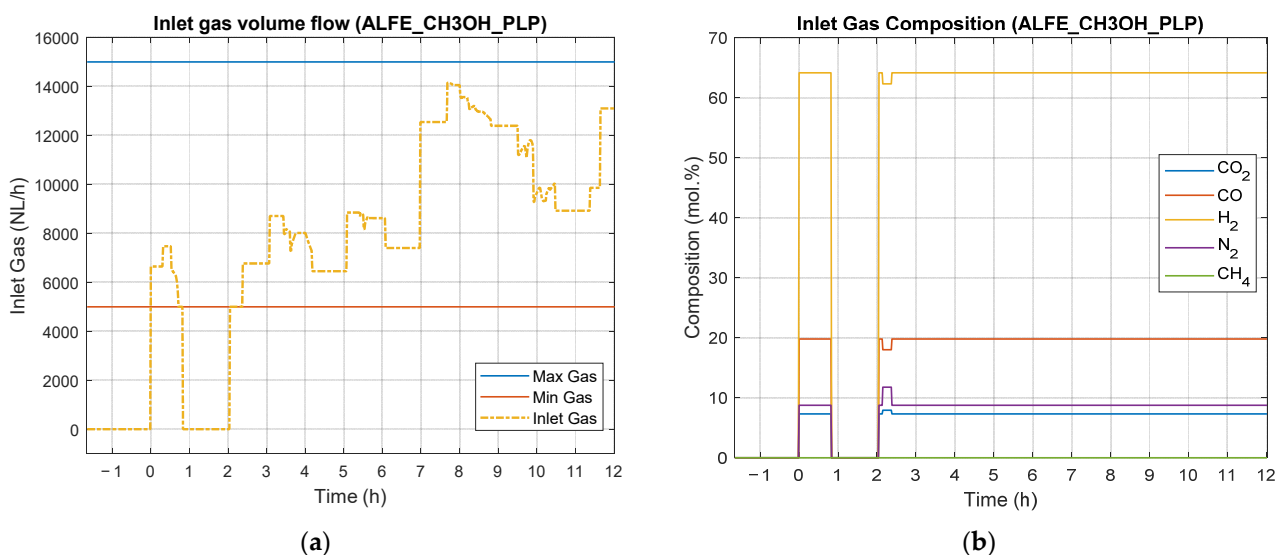

Figure 13. SC2. Control strategy for ALFE_CH3OH_PLP. (**a**) Inlet gas volume flow; (**b**) inlet gas composition.

In SC2, FAU_CH4_TR and ALFE_CH3OH_PLP worked in parallel. Moreover, in this case, the control action calculated by the DC forced the reactors to work in a complementary way. FAU_CH4_TR operated with an inlet gas composed of a mixture of BFG and hydrogen, while during the disturbance period, the reactor exploited mixed gas modalities (a mixture of BFG/BOFG enriched with hydrogen) to produce methane. On the other hand, the ALFE_CH3OH_PLP exploited BOFG and hydrogen as a unique inlet gas source. For very short periods during the disturbance in BFG availability, the methanol reactor exploited a mixture of BOFG and hydrogen with a small addition of BFG. Moreover, in this case, an estimate was calculated for the CO_2 reduction by summing the reduction contribution related to the use in the power plant of produced CH_4 in place of POGs and by considering the avoided emissions due to the production of CH_3OH. The CO_2 reduction results of about 774 t, corresponding to about 61% of those emitted in the case of burning the same amount of POGs exploited in the synthesis reactors directly in the power plant. An electrical energy production about 1.52 times higher was also obtained.

To sum up, the DC showed the capability to successfully react to disturbances in the main POG network while still allowing the correct operations of reactors. In addition, it also ensured significant benefits in terms of CO_2 emission reductions.

4.2. Results of Experimental Campaign with FAU_CH4_TR

As described in Section 4.1, the two methanation plants FAU_CH4_TR and MUL_CH4_TR were operated in parallel in SC1. The two phases of dynamic operation specified by the DC (approx. 0.5–2.5 h and 6.5–8.5 h without considering the warm-up phase) could be observed in the operation of FAU_CH4_TR (see Figure 14, solid lines). The dynamics involved transients in the volume flow rate ($\dot{V}_{tot}$) and gas composition. Five operating points (OP) for the evaluation were defined (see Table 2). OP1.1, OP1.3, and OP1.5 represent stoichiometrically adjusted BFG while OP1.2 and OP1.4 represent stoichiometrically adjusted mixtures of BOFG (main part) and BFG.
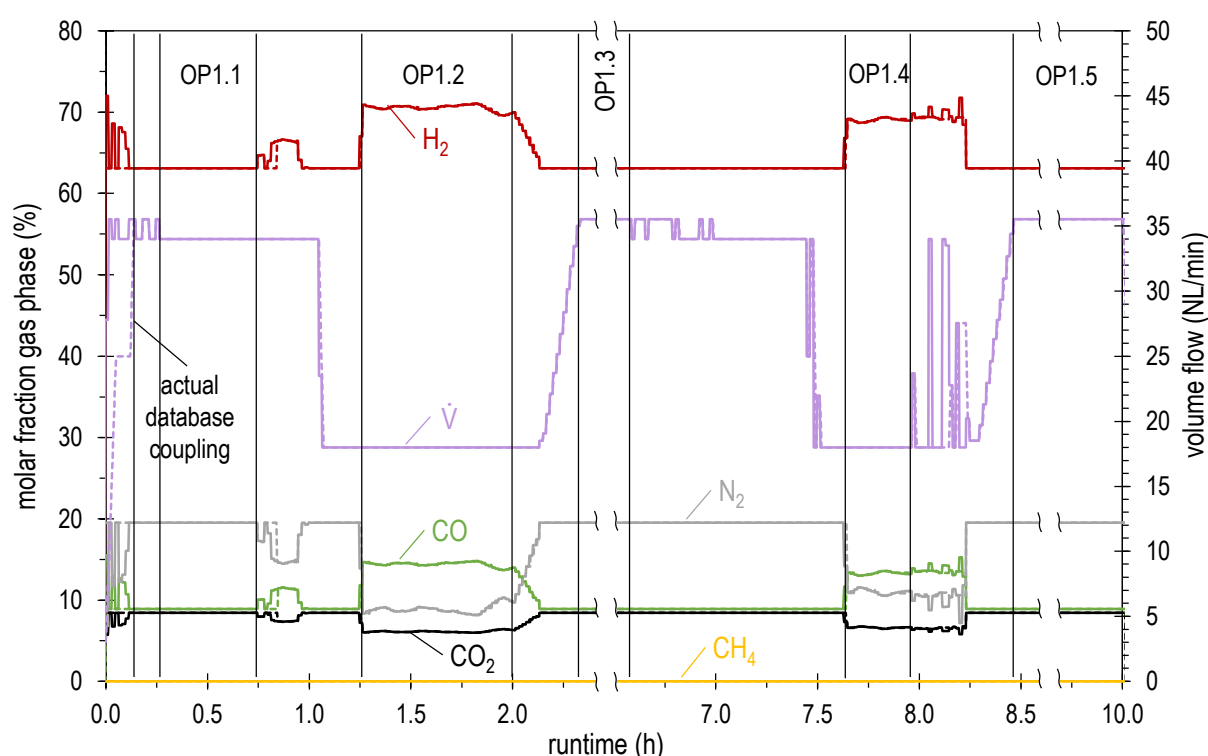
Figure 14. SC1. Handover values received from DC (solid lines) and set values of MFC (dashed lines) for FAU_CH4_TR.

Table 2. FAU_CH4_TR operating points defined for the evaluation; mean set values specified by the DC. p = 4 bar for all operating points.

Operating Point	$\dot{V}_{tot}$	H_2	CO_2	CO	CH_4	N_2	SN_{CH4}	P_{syn}
	NL/min	mol.%	mol.%	mol.%	mol.%	mol.%	-	kW
OP1.1	34.0	63.1	8.5	8.9	0.0	19.5	1.04	4.39
OP1.2	18.0	70.5	6.2	14.4	0.0	8.9	1.04	2.71
OP1.3	35.5	63.1	8.5	8.9	0.0	19.5	1.04	4.59
OP1.4	18.0	69.0	6.6	13.3	0.0	11.0	1.04	2.65
OP1.5	35.5	63.1	8.5	8.9	0.0	19.5	1.04	4.59
OP2.1	35.5	63.1	8.5	8.9	0.0	19.5	1.04	4.59

SC2 included the parallel operation of FAU_CH4_TR and ALFE_CH3OH_PLP. For FAU_CH4_TR, it comprised only one phase of dynamic operation (approx. 0.5–2.25 h, without considering the warm-up phase). Since the gain in knowledge was rather small compared to SC1, only one operating point is defined here for evaluation (see Table 2) OP2.1 represents stoichiometrically adjusted BFG.

Figure 14 compares the data received from DC to the set values of the mass flow controllers (MFC) for SC1. The latter (dashed lines) follow the specified values of the DC (solid lines) at almost every point during the 10 h of the experiment. Both gas volume flow and composition changes were automatically adopted by the PLC. However, there are exceptions where the graphs are not congruent. These deviations resulted from the implemented security query regarding the permitted stoichiometric limits, as some datasets were not forwarded to the MFC. This was caused by rounding errors in data processing resulting in calculated stoichiometric ratios smaller than 1.04. As a short-term corrective measure during the experiment, the corresponding values were typed in manually. After the experiment, the number of significant digits of rounding was increased, and the lower limit of the safety function checking the stoichiometry was slightly lowered.

Furthermore, the comparison of the data stored in the database by the DC and the received values recorded by the test rig's PLC showed that all datasets were transferred completely and without loss.

The temperature trends over the runtime for selected measurements in the structured reactor during SC1 are depicted in Figure 15. At the beginning of OP1.1, the influence of the reactor start-up phase can be clearly seen. The temperatures stabilized during this operating point, as the syngas power was relatively high (P_{syn} = 4.39 kW) and active cooling was applied. Between OP1.1 and OP1.2, the influence of the short switch in gas composition and the following decreasing volume flow ramp (see Figure 14) can be noticed. The temperature level did not stabilize during OP1.2 (CO-rich feed gas and low volume flow) despite stopping active cooling. For a longer operation of the structured reactor at this operating point, additional trace heating would have to be applied. During the start of OP1.3 (stoichiometrically adjusted BFG and high syngas power), the temperature rose again and was stabilized by active cooling at a desirable overall temperature level. The temperature over runtime for OP1.4 showed a behavior similar to OP1.2, as the conditions were almost the same. OP1.5 was identical to OP1.3, but the temperature stabilization this time did not succeed as fast as before.
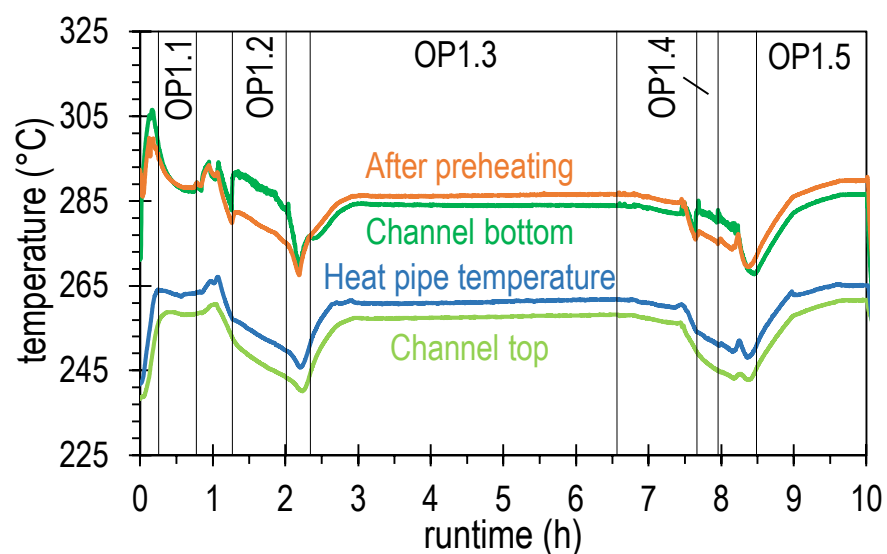

Figure 15. SC1. Temperature over runtime for selected measurements in the structured reactor of FAU_CH4_TR.

The curves in Figure 15 and the above-described dependencies clearly show that permanent monitoring and, if necessary, adjustment of the heat management (cooling and trace heating) is essential for the stable operation of the methanation system. These adjustments were made manually, despite the automated value transfer for the feed. In further development for the demonstration of a possible application in an industrial environment, a fully automated control concept will be required to take over this task.

Figure 16 illustrates the averaged axial temperature profiles of the structured reactor for the operating points OP1.3 and OP1.5. These showed a pronounced polytropic pattern with a temperature maximum of $\approx$500 °C about 48 mm after the start of the reaction channel. The maximum temperature was, thus, $\approx$200 °C lower than the expected adiabatic synthesis temperature and 50 °C lower than the maximum catalyst temperature. After the hotspot, the temperature declined to 265 °C at the reactor outlet, which increased the methane yield, $Y_{CH4,COx}$. The two requirements for an active cooling concept formulated in [53] (the limitation of the hotspot temperature to a high but materially acceptable level and a lowered outlet temperature) are, thus, met. The additionally plotted temperatures at the wall of a reaction channel (squares in Figure 16) clearly illustrate the large radial temperature gradient of up to 75 °C/mm. As the profiles of OP1.3 and OP1.5 are almost identical, it can be stated that same reaction and temperature conditions were reached during these operating points. Furthermore, the 12 individual profiles recorded at OP1.3 were completely congruent. The absence of a progressive change in temperature conditions in the structured reactor indicates that there was no change in the catalyst activity and, thus, no on-going catalyst deactivation.
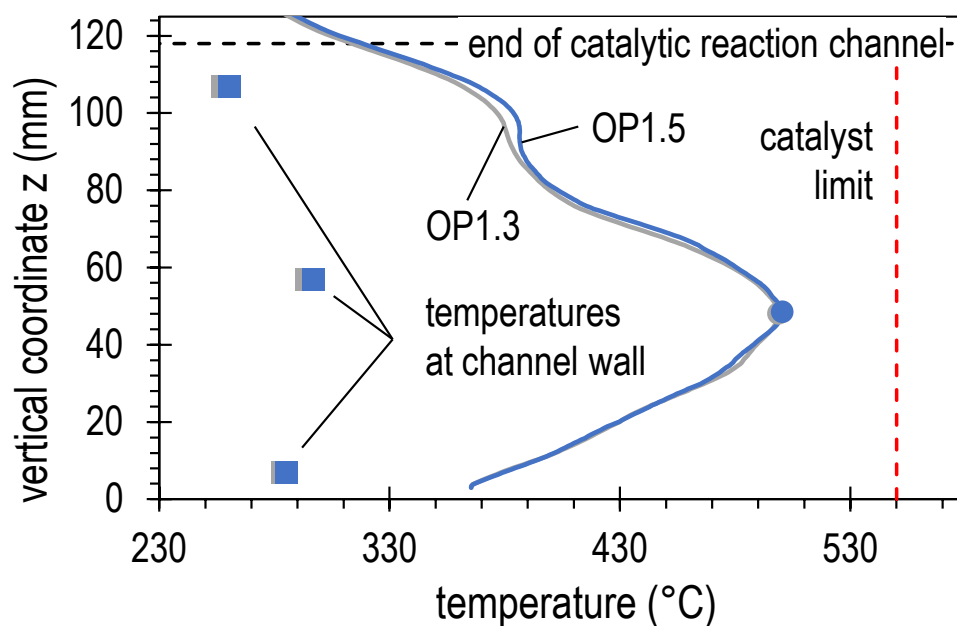

Figure 16. SC1. Axial temperature profiles (average) of the structured reactor of FAU_CH4_TR.

A summary of the evaluation of the hydrogen conversion, X_{H2}, and methane yield, $Y_{CH4,COx}$, is reported in Figure 17 for the five operating points of SC1. At the three comparable operating points, OP1.1, OP1.3, and OP1.5, full methane yield was achieved after the two-stage process with intermediate water separation. The hydrogen conversion was around 94.5% (over-stoichiometric feed gas composition). For OP1.2 and OP1.4, similar values for the final product gas are to be expected, but no product gas measurement was made after the second reactor stage at these points. The X_{H2} and $Y_{CH4,COx}$ of OP1.2 and OP1.4 (CO-rich gases and lower syngas power) after the first stage were higher ($\approx$6.5%) than the values at the operating points with equal amounts of CO and CO_2 and higher volume flow rates. A methane yield of around 91% was achieved in just one reactor stage.

The lower volume flow allowed a longer residence time in the catalyst bed. In addition, the reactants had a higher reactivity due to the increased CO content. These dependencies indicate a kinetic limitation in the structured reactor under the given conditions.
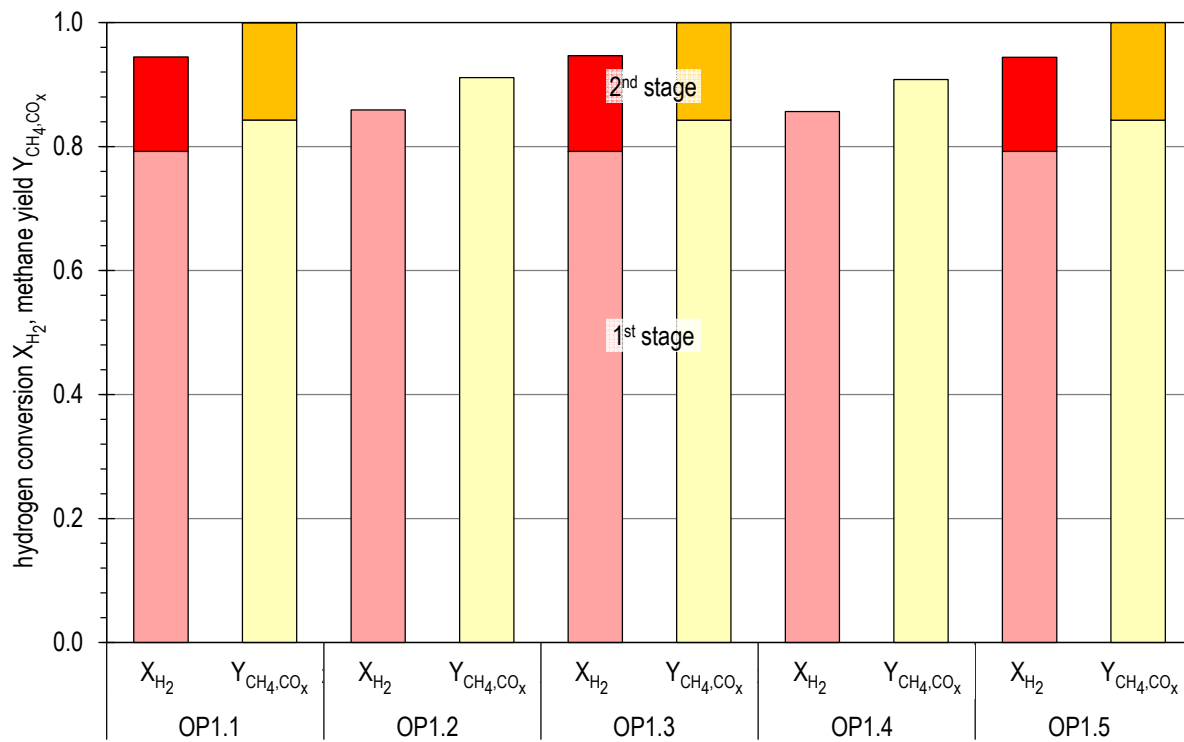

Figure 17. SC1. Hydrogen conversion, X_{H2}, and methane yield, $Y_{CH4,COx}$, after first and part of second methanation stage for the different operating points of FAU_CH4_TR.

Concerning SC2, Figure 18 shows the graphs of the data received from the DC in comparison to the set values of the MFC. Analogously to SC1, all datasets were completely and correctly transferred from the DC to the control system of the test rig. Nevertheless, noticeably in the dynamic part, some datasets did not comply with the reactor operating limits. The syngas power was too high at these points, and the programmed safety mechanisms skipped them. This greatly reduced the dynamics. The optimization tool should only calculate operating points that can also be run with the test rig. However, the maximum volume flows for BFG and BOFG, equivalent to meet the maximum syngas power with these gases, were stored in the DC models. Since the variation from 0.5 to 2.0 h in Figure 18 involved a mixture of both of these gases, there were probably deviations in calculating the maximum allowed volume flow of this mixture and thus the allowable syngas power was exceeded.

During the subsequent operating point, OP2.1, steady-state temperature conditions were achieved in the structured reactor and stationary gas compositions in both the intermediate and final gas. After the two-stage process, a full methane yield was achieved again with a hydrogen conversion of about 93.5%. This is in agreement with the values of comparable operating points from SC1 (see Figure 17).

4.3. Results of Experimental Campaign with MUL_CH4_TR

As described in Section 4.1 the operating parameters provided by the DC for MUL_CH4_TR in SC1 were mainly characterized by BOFG with highly dynamic fluctuations through jumps and impulses, ramps, and smooth changes. Nevertheless, the input gas composition was kept constant for each gas type, including a consistent hydrogen surplus of 4% (SN_{CH4} = 1.04). Such an excess in hydrogen compared to the reaction stoichiometry

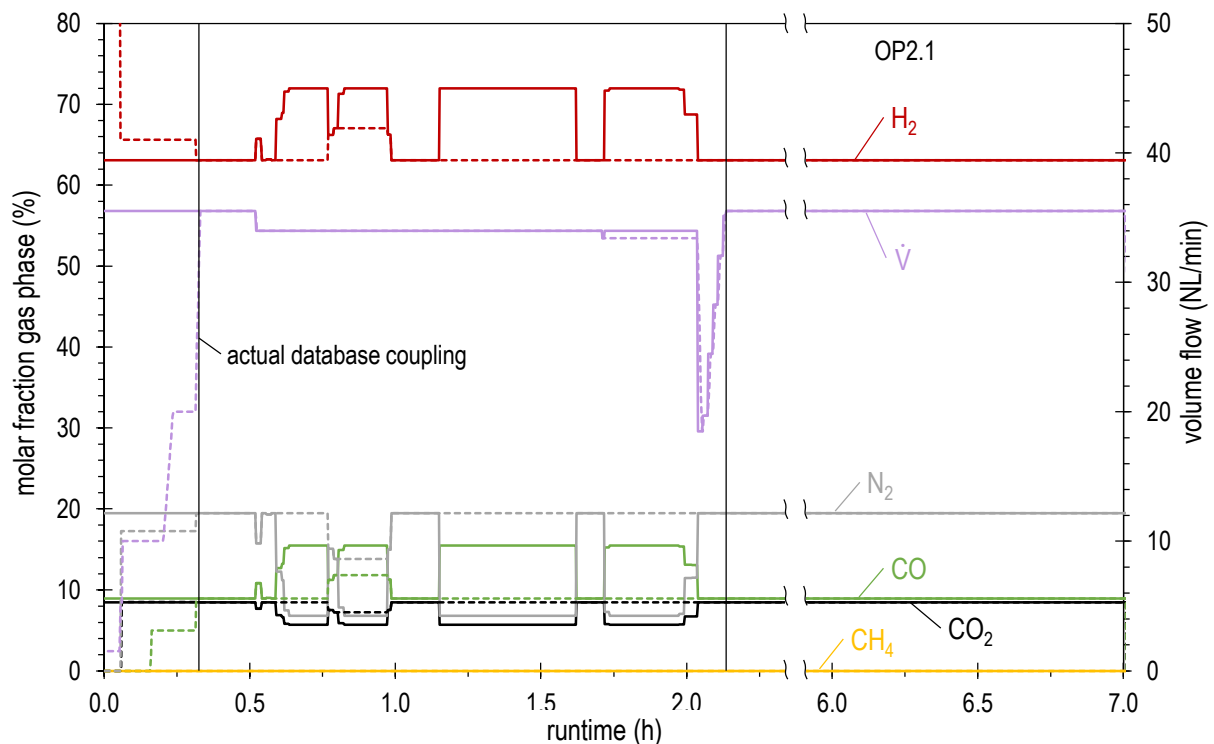(Equation (6)) met the optimum parameter for a methanation setup as used during the live experiments [60].

Figure 18. SC2. Handover values received from DC (solid lines) and set values of the MFC (dashed lines) for FAU_CH4_TR.

Prior to the start of methanation, the three reactors were heated up following the design specifications given by the catalyst manufacturer. The methanation of BOFG started with very smooth changes in the total volumetric flow rate, varying between 13.5 and 14 NL/min ($\approx$3200–3350 h^{-1} *GHSV*, 0 h). After 45 min, the flow rate increased to 18 NL/min ($\approx$4300 h^{-1} *GHSV*) over a period of 15 min and stayed at this elevated level for 5 h. During this period, multiple step increases, jumps in the total flow rate in the range of 2–3 NL/min were observed from one data point to the next one, representing a $\pm$16.7% increase in gas input power within 1 min. Furthermore, four changes to the BFG composition occurred instantly. These disturbances lasted for 4, 5, 14, and 2 min and resulted in a decrease in gas input power of up to 59.1%. Again, a consistent hydrogen surplus of 4% was guaranteed during the BFG disturbances. The second half of the live experiment was again characterized by a high usage of BOFG at about 18 NL/min, including step changes in the total volume flow as well as one disturbance with BFG. After a period of 1.5 h without any changes, the maximum flow rate of the live experiments of 22.5 NL/min was reached. The increase was achieved through imminent changes in the range of 1–2 min. During the whole duration of the experiment, a constant pressure of 4 bar was kept, meeting the specifications of the steelworks plant.

Figure 19 shows the time-based data for the following parameters: *GHSV* and product gas compositions for CH_4, H_2, CO, and CO_2 measured after the third reactor (N_2 = rest to 100%) as well as the CO_x conversion rate. Sixteen representative operating points are highlighted with black dots flagging dynamic changes in critical parameters.
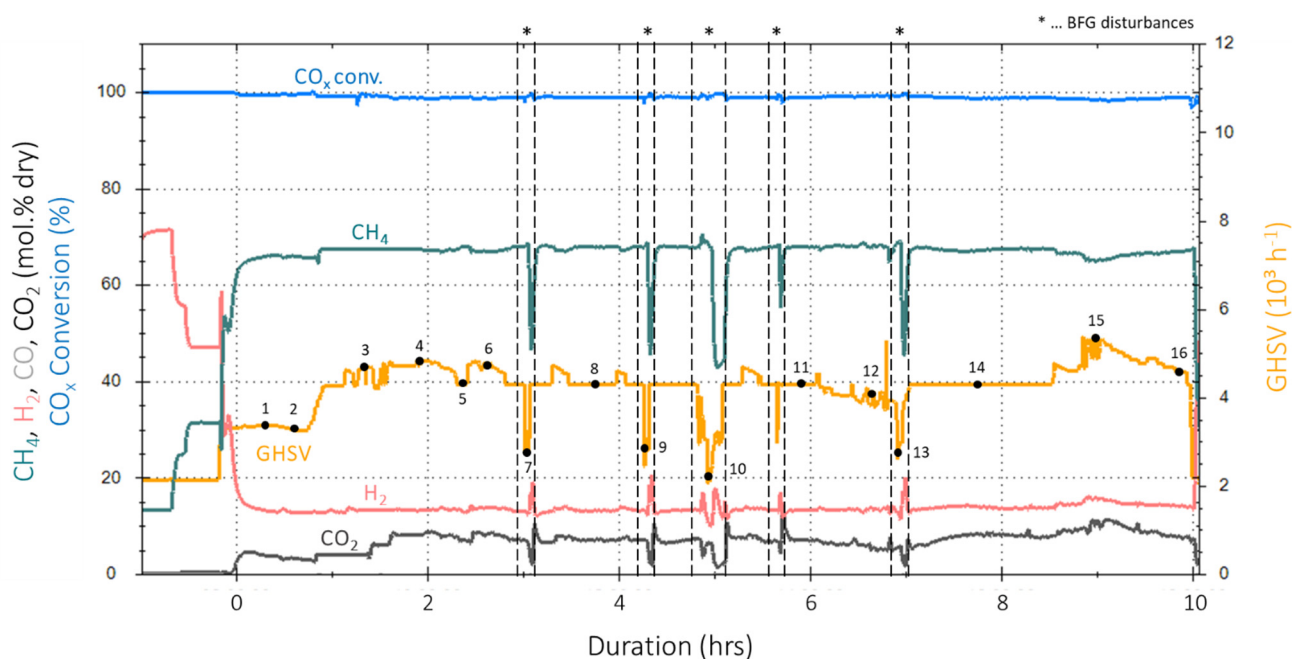
Figure 19. SC1. Time-based data for live experiments with MUL_CH4_TR: gas composition in mol.% (dry), CO_x conversion in %, and *GHSV* in $10^3\ h^{-1}$; sixteen representative operating points are marked with black dots.

Although highly dynamic variations in BOFG input power up to 45% were performed, the product gas composition measured after the third reactor stage remained nearly constant. The individual gas components, H_2, CO_2, CO, CH_4, and N_2, varied within a $\pm 2.8\%$ pt. range around their averages. Figure 20 gives an overview of the detailed gas composition for the 16 reference points, each representing a relevant dynamically changing operating condition. Hydrogen varied between 12.7 and 15.4 mol.% (dry), and methane stayed between 65.2 and 70.1 mol.% (dry). The concentration of CO_2 remained at a very low level of about 0.7 mol.% (dry) on average. As no CO was measured in the product gas, the CO_x conversion constantly remained, on average, above 99.0% (see Table 3).

The results of the instant changes from BOFG to BFG were noticeable. The CO_x conversion increased during these changes (#7, 9, 10, and 13), as the blue curve in Figure 19 and the values in Table 3 indicate; this was due to the lower flow rates and related *GHSV* and the resulting longer residence times. With an optimized temperature control of the reactors, conversion rates of up to 99.8% were achieved. Furthermore, the product gas composition changed to $\approx 47\%$ for CH_4, $\approx 17\%$ for H_2, and $\approx 36\%$ for N_2 due to the different injected gas compositions. Verification experiments carried out after the live experiment did not indicate any signs of catalyst deactivation due to the highly dynamic changes in operating conditions.

4.4. Results of Experimental Campaign with ALFE_CH3OH_PLP

The methanol synthesis experiments during SC2 were conducted in ALFE_CH3OH_PLP with a commercial methanol catalyst filled in the four stages of the multi-stage setup. The use of the control tool described in Section 3.4. in real time to provide set points for ALFE_CH3OH_PLP considering the use of POGs was demonstrated. Methanol was successfully produced under fluctuating conditions, and the test served as a proof of concept for advanced process control with synthetic gas mixtures and load profiles provided by the DC through an online connection.
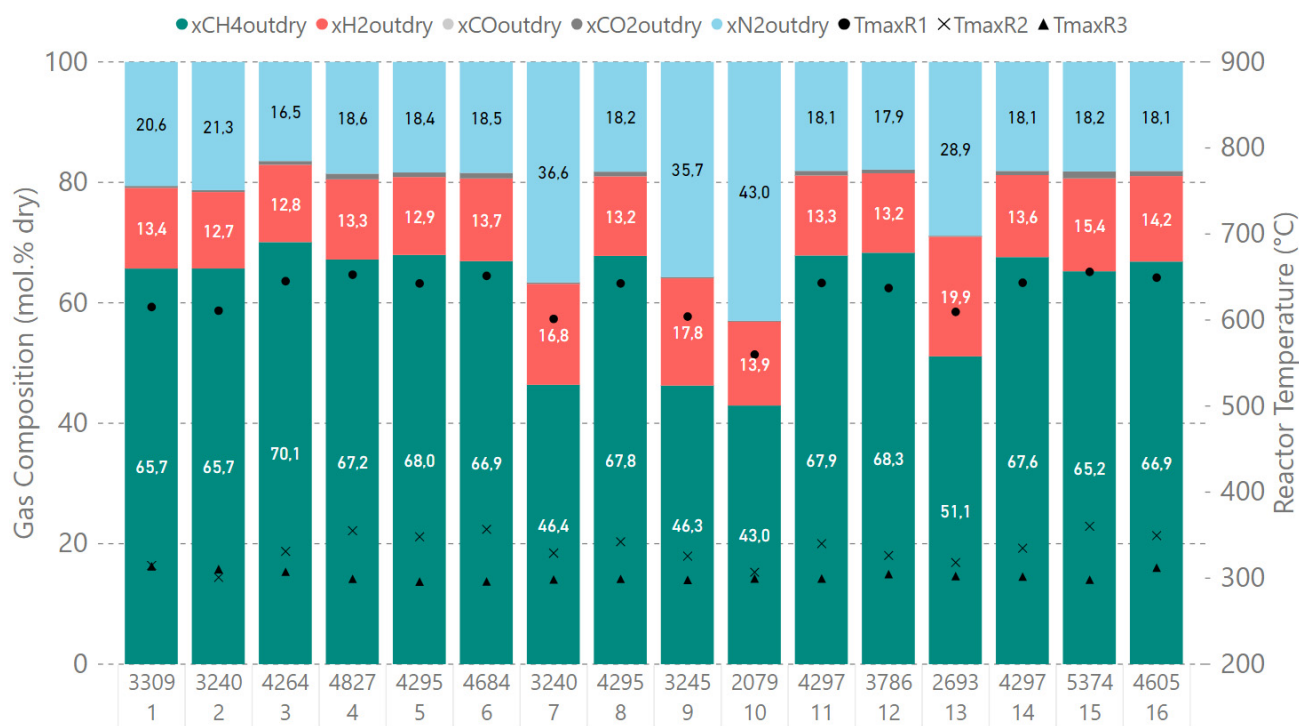
Figure 20. SC1. Product gas compositions and max. reactor temperatures for 16 representative points in time (values in mol.% (dry) and °C) for MUL_CH4_TR.

Table 3. SC1. Operating parameters, product gas compositions, and CO_x conversion (X_{COx}) rates for 16 representative dynamic operating points for MUL_CH4_TR. BFG disturbances are highlighted with *. SN_{CH4} = 1.04 for all reference points.

Operating Point	$\dot{V}_{tot}$	GHSV	H_2	CO_2	CO	CH_4	N_2	X_{COx}
	NL/min	h^{-1}	mol.%	mol.%	mol.%	mol.%	mol.%	%
1	13.9	3300	13.4	0.3	0.0	65.7	20.6	99.6
2	13.6	3200	12.7	0.3	0.0	65.7	21.3	99.6
3	17.9	4300	12.8	0.6	0.0	70.1	16.5	99.2
4	20.2	4800	13.3	1.0	0.0	67.2	18.6	98.7
5	18.0	4300	12.9	0.8	0.0	68.0	18.4	98.9
6	19.6	4700	13.7	0.9	0.0	66.9	18.5	98.7
7 *	18.0	3200	16.8	0.3	0.0	46.4	36.6	99.5
8	18.0	4300	13.2	0.8	0.0	67.8	18.2	98.9
9 *	18.0	3200	17.8	0.2	0.0	46.3	35.7	99.6
10 *	12.3	2100	13.9	0.2	0.0	43.0	43.0	99.7
11	18.0	4300	13.3	0.8	0.0	67.9	18.1	98.9
12	15.9	3800	13.2	0.6	0.0	68.3	17.9	99.2
13 *	16.3	2700	19.9	0.2	0.0	51.1	28.9	99.8
14	18.0	4300	13.6	0.7	0.0	67.6	18.1	99.0
15	22.5	5400	15.4	1.2	0.0	65.2	18.2	98.3
16	19.3	4600	14.2	0.8	0.0	66.9	18.1	98.8

As described in Section 4.1., FAU_CH4_TR and ALFE_CH3OH_PLP simultaneously received information from the DC and ran in parallel to produce methane and methanol. Hence, 10 points were tested at ALFE under fluctuating conditions to successfully and effectively produce methanol as set points were received through the online connection in real time from the DC. The high flexibility of the plant and the dedicated analytics allowed the plant to respond very quickly and effectively to load variations.

A typical BOFG composition was used together with additional H_2 to adjust the SN_{CH3OH} to 2.1. A once-through operation was chosen to lower the plant response time regarding new parameters for the synthesis. This allowed quick adaptation to load changes. The composition of the feedstock for the methanol synthesis was:

CO_2: 7.3 mol.%;

CO: 19.8 mol.%;

H_2: 64.2 mol.%;

N_2: 8.7 mol.%.

The temperatures and pressures during the synthesis were adapted to the changes in load, and the online analysis gave rapid information on conversions and stream compositions at the reactor outlet. Particular attention was given to combine high conversions with moderate temperature profiles to limit by-product formation.

Figure 21 describes the different loads provided in real time by the DC (black) and demonstrates very clearly the fast response of the unit to these variations (red). The time between the decision on a new set point and the process value of the flow controller was very fast, and the desired set point was reached in a few minutes.
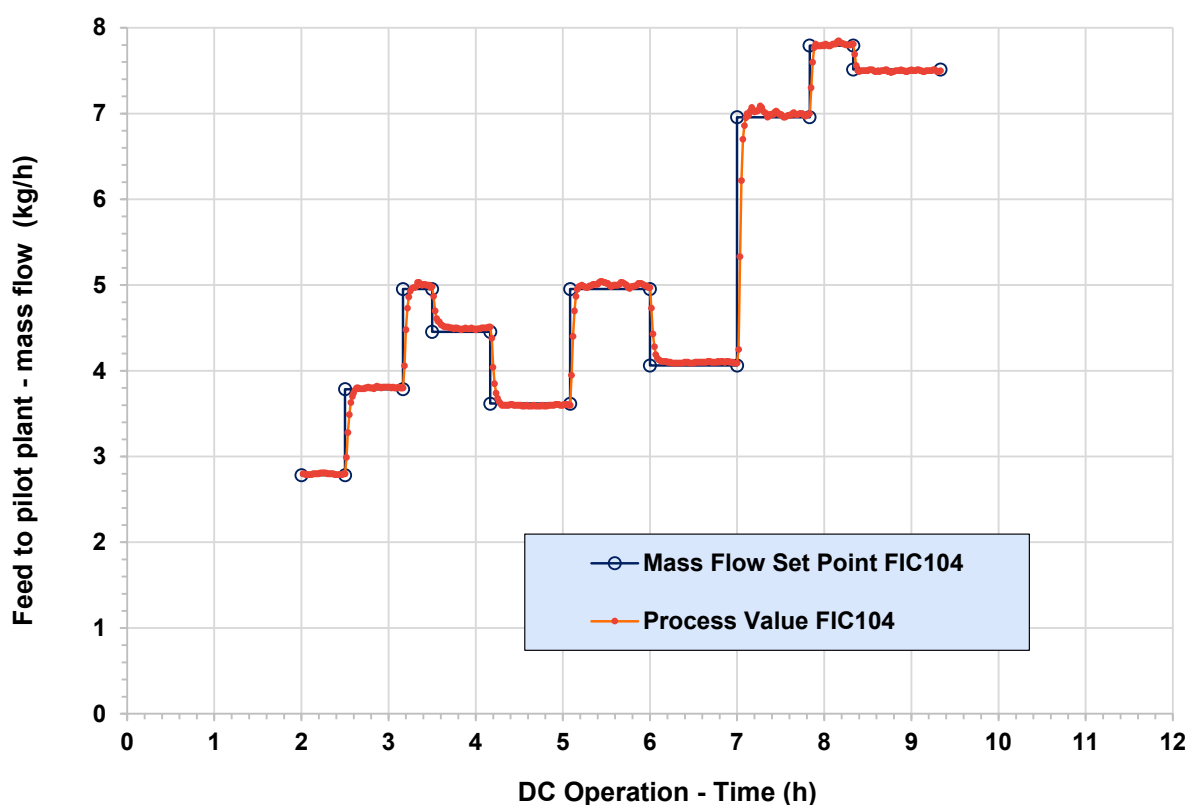

Figure 21. SC2. Mass flow set points versus time during test campaign of ALFE_CH3OH_PLP with DC.

In a deviation from the inlet conditions for the pilot plant shown in Figure 13, the operators did not start the methanol production from the very first values suggested by the DC (time 0 in Figures 13 and 21) but only after two hours of DC operation. The stop-and-go operation was not part of this test campaign at ALFE. Moreover, a certain smoothing of the load profile was performed (see comparison Figures 13a and 21), and only one gas composition (as mentioned above) was used.

The results in terms of catalytic performance were good and in accordance with expectations. The CO conversion (X_{CO}) for each load and without any recycling was always higher than 99% and in most of the cases overcame 99.5%. The CO_2 conversion (X_{CO2}) was also high but still lower than for CO. In more detail, CO_2 conversions were

between 70% and 78% during the campaign depending on the amount of feed entering the synthesis section. This was expected, as CO_2 is well-known to be more difficult to be converted in one pass compared to CO at mild conditions for methanol synthesis. Nevertheless, CO_2 conversion can be increased by optimizing the operating conditions, especially acting on temperatures and pressures.

By increasing loads, the amount of methanol produced was also increased accordingly, even if slightly lower CO and CO_2 conversions were observed, as shown in Table 4. The flexibility of ALFE_CH3OH_PLP and the dedicated analytics ensured a quick unit adaptation, even when the load was rapidly increased or decreased. The plant flexibility was also guaranteed by the deep control of temperature (see Section 3.3) that provided valuable real-time information to the operators.

Table 4. SC2. Catalytic performance in the four-stage reactor system ALFE_CH3OH_PLP under once-through conditions.

Time of Sampling	p	T	T_{max}	Feed	X_{CO2}	X_{CO}	X_{H2}	Raw CH$_3$OH
hours	bar	°C	°C	NL/h (kg/h)	%	%	%	kg/h
2.00 (start of operation)	80	220	278	4927 (2.80)	77.8	99.6	82.5	2.06
2.80	80	220	272	6530 (3.71)	77.3	99.6	79.7	2.72
3.30	80	220	269	8441 (4.79)	77.7	99.6	80.2	3.52
3.80	80	220	269	8000 (4.54)	76.4	99.6	79.2	3.32
4.50	80	220	272	6459 (3.66)	76.3	99.6	81.1	2.67
5.30	80	220	269	8663 (4.91)	75.0	99.5	78.8	3.56
6.30	80	230	280	7323 (4.15)	74.3	99.4	79.2	2.99
7.30	80	230	273	11,945 (6.78)	72.6	99.2	77.6	4.85
8.00	80	230	271	13,618 (7.73)	70.5	99.1	77.0	5.47
9.50 (end of operation)	80	230	271	13,265 (7.52)	70.4	99.1	78.3	5.32

The amount of by-products was still lower than 5000 wt.ppm despite the high CO concentration and the high maximum temperature in the first stage (see Table 5). The by-product concentration in raw methanol decreased when the feed amount increased for a given gas composition. The by-product amount lied in a range that can be covered by a traditional distillation section to produce a commercial methanol suitable for the market without additional treatment.

Table 5. SC2. By-product amount in raw methanol from ALFE_CH3OH_PLP at different feed amounts.

Time of Sampling	p	T	T_{max}	Feed	Raw CH$_3$OH	Water in Raw CH$_3$OH	Total By-Products
hours	bar	°C	°C	NL/h (kg/h)	kg/h	%	wt.ppm
2.00 (start of operation)	80	220	278	4927 (2.80)	2.06	11.8	4680
9.50 (end of operation)	80	230	271	13,265 (7.52)	5.32	10.9	4460

In both cases, low load and high load, it can be observed in Tables 6 and 7 that the high conversion of CO in the first stage also led to higher maximum temperatures in the catalytic bed. This caused the formation of a high amount of by-products in the first stage. The CO_2 conversion was much lower in the first stage than the conversion of CO and, as a consequence, the concentration of water in the raw methanol produced in the first stage

was low. The amount of by-products produced in the first stage could be compensated by the lower production of by-products at later stages, and this delivered a collected and gathered final raw methanol product that was able to be purified in the distillation section.

Table 6. Conversion of CO_2, CO, and H_2 in each stage and for the overall plant at low load (4927 NL/h (2.80 kg/h)) in the four-stage methanol plant (T = 220 °C, p = 80 bar); time of sampling: 2.00 h (start of operation).

Stage	Feed Inlet	T_{inlet}	T_{max}	X_{CO2}	X_{CO}	X_{H2}	By-Products in Raw MeOH	Water in Raw MeOH
-	NL/h	°C	°C	%	%	%	wt.ppm	wt.%
1	4927	220	278	16.9	93.0	56.9	6450	3.2
2	2132	220	226	40.3	84.4	29.5	671	27.5
3	1557	220	224	50.9	52.1	24.1	396	35.6
4	1236	220	224	60.0	41.1	21.6	339	35.7
Overall Plant	4927	220	278	77.8	99.6	82.5	4680	11.8

Table 7. Conversion of CO_2, CO, and H_2 in each stage and for the overall plant at high load (13,265 NL/h (7.52 kg/h)) in the four-stage methanol plant (T = 230 °C, p = 80 bar); time of sampling: 9.50 h (end of operation).

Stage	Feed Inlet	T_{inlet}	T_{max}	X_{CO2}	X_{CO}	X_{H2}	By-Products in Raw MeOH	Water in Raw MeOH
	NL/h	°C	°C	%	%	%	wt.ppm	wt.%
1	13,265	230	271	13.1	82.3	49.7	6463	2.5
2	6656	230	243	26.9	82.1	29.3	1258	17.2
3	4802	230	236	38.9	58.0	22.4	519	32.8
4	3854	230	236	47.0	44.7	20.0	387	35.4
Overall Plant	13,265	230	271	70.4	99.1	78.3	4460	10.9

This means that CO_2-rich gases can be used as well as CO-rich gases in this type of equipment, which is a perfect complement to the dispatch controller, which distributes in real time the different loads and different compositions of steelworks off-gases to convert them into methanol and/or methane.

The amount of feed and the gas composition entering the first stage was provided by the dispatch controller as described in Tables 6 and 7. The outlet of the first stage was then separated into a liquid phase that represented the raw methanol and a gas phase that was sent as a feed to stage 2. This process was then repeated for all the stages, as already explained in Section 3.3 of this publication. Therefore, the gas composition as well as the amount of feed at the stage inlet were different for all the stages. As a consequence, the amount of raw methanol produced also differed. Hence, the raw methanol produced after each stage was removed, gathered, and sent to a low-pressure separator, which separated the solved gases from the final raw methanol product.

The overall conversions of CO for the different loads were above 99% but were slightly better for the lower amount of feed and lower inlet temperatures. The conversion of CO_2 was more sensible to the amount of feed entering the reactor, with an overall CO_2 conversion of 70.4% for the high-load test point in comparison to 77.8% for the low-load test point, even if the temperature was 10 °C lower in this case (220 °C for low-load test versus 230 °C for high-load test). The control of the maximum temperature in the different stages in real time was very important to avoid severe degradation of the catalyst.

The same exercise can be conducted with different compositions of BFG, BOG, COG, and/or mixture of these gases, and the plant can perform well, producing a suitable amount of methanol with limited by-product volume. The control of gas compositions and available hydrogen are key parameters. Nevertheless, ALFE_CH3OH_PLP can adapt

to a low hydrogen amount and to a high amount of inerts in the feed, ensuring suitable methanol production.

Moreover, ALFE_CH3OH_PLP can be put in a stand-by condition and started and stopped without any significant issue. No loss of performance and no unusual deterioration of the catalyst were observed during a further extended test campaign of about 1800 h on a stream with different gas compositions representing POGs. The 1800 h on the stream included the commissioning and validation phase of the pilot plant with well-known gas compositions and operating conditions as well as several test points at a steady state with synthetic steel gas mixtures as the feed for the methanol synthesis. In this publication, exclusively the results linked to the test under dynamic conditions with a direct coupling to the developed dispatch controller are described.

5. Summary, Conclusions, and Future Works

The work and tests reported in this paper concern the design and construction of a complex, virtually coupled test rig consisting of several synthesis reactors for the production of methane and methanol located in three different locations (one in Austria and two in Germany), a remote computing, supervision, and control system located in Italy, and a data processing system that allows the distribution of measurements, simulated data, and control strategies between the systems of interest.

The carried out online tests have shown that the calculation, optimization, and control architecture can lead to promising and satisfying results. First of all, the data exchange architecture based on an OPC UA infrastructure allowed the distribution of measures and control strategies to several recipients in parallel without transmission/reception issues. The control and supervision system, namely, the dispatch controller (DC), allowed the calculation of control strategies in real time with a temporal resolution of one minute and sufficiently smooth and optimal/sub-optimal control trends in the pre-established time. The optimization problem formulated as a non-linear MILP, linearized in real time, allowed the description of the dynamic behavior of the reactors and of all the equipment connected to the methane/methanol production system with sufficient accuracy.

The operation of the three synthesis reactors with steelworks process off-gases ran without errors for the two scenarios presented. Two plants each were operated in parallel over periods of 10 and 7 h, respectively, with values that were specified by the DC and distributed to the plants or their operators via an OPC UA.

FAU's bench-scale methanation test rig received the DC's specified values directly via the OPC UA and processed them automatically. The safety routines implemented for this purpose worked reliably, albeit in part with very strict limit specifications. The two-stage methanation with a structured fixed-bed reactor as the first stage responded quickly to specified load or feed gas composition changes with a stable operating behavior and a high reproducibility of results. A full methane yield was obtained after the two-stage methanation with intermediate water separation, of which up to 91% could already be achieved in the first reactor stage. No evidence of progressive catalyst deactivation was observed.

MUL's bench-scale methanation plant also showed resilient behavior to the load fluctuations specified by the DC. Even with quick and large changes in input power of up to 45%, the product gas composition remained almost constant after the three-stage process. Consistently high CO_x conversion rates of over 99% on average were achieved. Moreover, no additional catalyst deactivation was noticeable.

ALFE's innovative multi-stage pilot plant for methanol synthesis showed high flexibility in once-through operation in terms of inlet gas composition and variable operating conditions. The plant reacted to a load change within minutes and always showed a stable operating behavior. Both the handling of a high content of inerts and unusual reactant gas mixtures (POGs, high N_2 content, and a mixture of CO and CO_2) were mastered, even under fluctuating conditions. CO and CO_2 conversions were over 99% and between 70–78%,

respectively. The amount of by-products was low for the prevailing reaction conditions (<5000 wt.ppm).

The results of the live coupling tests via online connection suggest that it is possible to integrate methane and/or methanol generation plants in combination with an intelligent supervision and control system into existing steelworks as a CCU concept while also obtaining significant advantages in terms of CO_2 emission reductions. However, further testing, for example, the live feedback of the real plants to the dispatch controller, the direct coupling of the plants to an electrolyzer, and a higher level of automation (automated value transfer and processing to/at all plants and an automated stabilization of operating points) are necessary before an on-site demonstration at a steelworks can take place.

Furthermore, future works will be aimed at investigating different topics, including a complete sensitivity analysis of the economic costs as a function of energy media and CO_2 prices. Further studies will focus on the more detailed computation of CO_2 reductions through the production of methane and methanol with the plants presented on an industrial scale and considering all the sources of avoided CO_2 (e.g., also those related to the extraction, preparation, and transportation of primary NG). In addition, an improvement in the dispatch controller will be studied through the implementation of more accurate models, including product treatment and cleaning equipment. In this sense, future works will probably also make it possible to refine the control strategies and/or the design of the plants to maximize their effectiveness.

Institutional Review Board Statement: Not applicable.

Informed Consent Statement: Not applicable.

Data Availability Statement: Not applicable.

Conflicts of Interest: The authors declare no conflict of interest.

References

1. European Commission. *The European Green Deal*; European Commission: Brussels, Belgium, 2019.
2. European Commission. *"Fit for 55": Delivering the EU's 2030 Climate Target on the Way to Climate Neutrality*; European Commission: Brussels, Belgium, 2021.
3. European Commission. *Towards Competitive and Clean European Steel*; European Commission: Brussels, Belgium, 2021.
4. Estep Clean Steel Partnership. *Strategic Research and Innovation Agenda (SRIA)*; Estep Clean Steel Partnership: Brussels, Belgium, 2021.

5. Voestalpine Stahl GmbH. *Analysenergebnisse Der Umwelt—Und Betriebsanalytik (Durchgeführt Für i3 Upgrade)*; Technical Report; Voestalpine Stahl GmbH: Linz, Austria, 2019.

6. Remus, R.; Roudier, S.; Aguado Monsonet, M.A.; Sancho, L.D. *Best Available Techniques (BAT) Reference Document for Iron and Steel Production*; Publications Office of the European Union: Luxembourg, 2013.

7. Schlüter, S.; Hennig, T. Modeling the Catalytic Conversion of Steel Mill Gases Using the Example of Methanol Synthesis. *Chem. Ing. Tech.* **2018**, *90*, 1541–1558. [CrossRef]

8. Razzaq, R.; Li, C.; Zhang, S. Coke oven gas: Availability, properties, purification, and utilization in China. *Fuel* **2013**, *113*, 287–299. [CrossRef]

9. Moral, G.; Ortiz-Imedio, R.; Ortiz, A.; Gorri, D.; Ortiz, I. Hydrogen Recovery from Coke Oven Gas. Comparative Analysis of Technical Alternatives. *Ind. Eng. Chem. Res.* **2022**, *61*, 6106–6124. [CrossRef] [PubMed]

10. Zhang, Q.; Li, Y.; Xu, J.; Jia, G. Carbon element flow analysis and CO2 emission reduction in iron and steel works. *J. Clean. Prod.* **2018**, *172*, 709–723. [CrossRef]

11. Bhaskar, A.; Assadi, M.; Somehsaraei, H.N. Decarbonization of the Iron and Steel Industry with Direct Reduction of Iron Ore with Green Hydrogen. *Energies* **2020**, *13*, 758. [CrossRef]

12. Wang, R.; Zhao, Y.; Babich, A.; Senk, D.; Fan, X. Hydrogen direct reduction (H-DR) in steel industry—An overview of challenges and opportunities. *J. Clean. Prod.* **2021**, *329*, 129797. [CrossRef]

13. Patisson, F.; Mirgaux, O. Hydrogen Ironmaking: How it Works. *Metals* **2020**, *10*, 922. [CrossRef]

14. Porzio, G.F.; Fornai, B.; Amato, A.; Matarese, N.; Vannucci, M.; Chiappelli, L.; Colla, V. Reducing the energy consumption and CO_2 emissions of energy intensive industries through decision support systems—An example of application to the steel industry. *Appl. Energy* **2013**, *112*, 818–833. [CrossRef]

15. Porzio, G.F.; Nastasi, G.; Colla, V.; Vannucci, M.; Branca, T.A. Comparison of multi-objective optimization techniques applied to off-gas management within an integrated steelwork. *Appl. Energy* **2014**, *136*, 1085–1097. [CrossRef]

16. Maddaloni, A.; Matino, R.; Matino, I.; Dettori, S.; Zaccara, A.; Colla, V. A quadratic programming model for the optimization of off-gas networks in integrated steelworks. *Matér. Tech.* **2019**, *107*, 502. [CrossRef]

17. Colla, V.; Matino, I.; Dettori, S.; Petrucciani, A.; Zaccara, A.; Weber, V.; Salame, S.; Zapata, N.; Bastida, S.; Wolff, A.; et al. Assessing the efficiency of the off-gas network management in integrated steelworks. *Matér. Tech.* **2019**, *107*, 104. [CrossRef]

18. Matino, I.; Dettori, S.; Castellano, A.; Matino, R.; Mocci, C.; Vannocci, M.; Maddaloni, A.; Colla, V.; Wolff, A. Machine Learning-Based Models for Supporting Optimal Exploitation of Process Off-Gases in Integrated Steelworks. In Proceedings of the Cybersecurity Workshop by European Steel Technology Platform, ESTEP 2020: Impact and Opportunities of Artificial Intelligence Techniques in the Steel Industry, Pisa, Italy, 15–16 October 2020; Springer: Cham, Switzerland, 2020; pp. 104–118.

19. Dettori, S.; Matino, I.; Colla, V.; Speets, R. A Deep Learning-Based Approach for Forecasting off-Gas Production and Consumption in the Blast Furnace. *Neural Comput. Appl.* **2022**, *34*, 911–923. [CrossRef] [PubMed]

20. Dettori, S.; Matino, I.; Colla, V.; Weber, V.; Salame, S. Neural Network-based modeling methodologies for energy transformation equipment in integrated steelworks processes. *Energy Procedia* **2019**, *158*, 4061–4066. [CrossRef]

21. Matino, I.; Dettori, S.; Colla, V.; Weber, V.; Salame, S. Forecasting blast furnace gas production and demand through echo state neural network-based models: Pave the way to off-gas optimized management. *Appl. Energy* **2019**, *253*, 113578. [CrossRef]

22. Rieger, J.; Colla, V.; Matino, I.; Branca, T.; Stubbe, G.; Panizza, A.; Brondi, C.; Falsafi, M.; Hage, J.; Wang, X.; et al. Residue Valorization in the Iron and Steel Industries: Sustainable Solutions for a Cleaner and More Competitive Future Europe. *Metals* **2021**, *11*, 1202. [CrossRef]

23. Chisalita, D.-A.; Petrescu, L.; Cobden, P.; van Dijk, H.; Cormos, A.-M.; Cormos, C.-C. Assessing the environmental impact of an integrated steel mill with post-combustion CO2 capture and storage using the LCA methodology. *J. Clean. Prod.* **2018**, *211*, 1015–1025. [CrossRef]

24. Huang, Z.; Ding, X.; Sun, H.; Liu, S. Identification of main influencing factors of life cycle CO2 emissions from the integrated steelworks using sensitivity analysis. *J. Clean. Prod.* **2010**, *18*, 1052–1058. [CrossRef]

25. Saima, W.H.; Mogi, Y.; Haraoka, T. Development of PSA System for the Recovery of Carbon Dioxide and Carbon Monoxide from Blast Furnace Gas in Steel Works. *Energy Procedia* **2013**, *37*, 7152–7159. [CrossRef]

26. Steynberg, A. Chapter 1—Introduction to Fischer-Tropsch Technology. In *Studies in Surface Science and Catalysis*; Steynberg, A., Dry, M., Eds.; Elsevier: Amsterdam, The Netherlands, 2004; Volume 152, pp. 1–63.

27. Valera-Medina, A.; Roldan, A. Ammonia from Steelworks. In *Sustainable Ammonia Production. Green Energy and Technology*; Inamuddin, Boddula, R., Asiri, A., Eds.; Springer: Cham, Switzerland, 2020; pp. 69–80.

28. De Ras, K.; Van De Vijver, R.; Galvita, V.V.; Marin, G.B.; Van Geem, K.M. Carbon capture and utilization in the steel industry: Challenges and opportunities for chemical engineering. *Curr. Opin. Chem. Eng.* **2019**, *26*, 81–87. [CrossRef]

29. Lyke, S.E.; Moore, R.H. *Chemical Production from Industrial By-Product Gases: Final Report*; Battelle Pacific Northwest Labs: Richland, WA, USA, 1981.

30. Cordier, J.; Dussart, B. Ammonia and Methanol Production—How Savings Can Be Made. *Pet. Technol.* **1984**, *307*, 38–45.

31. Kim, S.; Kim, J. The optimal carbon and hydrogen balance for methanol production from coke oven gas and Linz-Donawitz gas: Process development and techno-economic analysis. *Fuel* **2020**, *266*, 117093. [CrossRef]

32. Deng, L.; Ii, T.A.A. Techno-economic analysis of coke oven gas and blast furnace gas to methanol process with carbon dioxide capture and utilization. *Energy Convers. Manag.* **2019**, *204*, 112315. [CrossRef]

33. Kim, D.; Han, J. Techno-economic and climate impact analysis of carbon utilization process for methanol production from blast furnace gas over Cu/ZnO/Al$_2$O$_3$ catalyst. *Energy* **2020**, *198*, 117355. [CrossRef]

34. Lundgren, J.; Ekbom, T.; Hulteberg, C.; Larsson, M.; Grip, C.-E.; Nilsson, L.; Tunå, P. Methanol production from steel-work off-gases and biomass based synthesis gas. *Appl. Energy* **2013**, *112*, 431–439. [CrossRef]

35. Haag, S.; Castillo-Welter, F.; Schuhmann, T.; Williams, B.A.; Oelmann, T.; Günther, A.; Gorny, M. How to Convert CO$_2$ to Green Methanol. In Proceedings of the Challenges for Petrochemicals and Fuels: Integration of Value Chains and Energy Transition (DGMK Conference), Berlin, Germany, 10–12 October 2018.

36. Oelmann, T.; Gorny, M.; Schuhmann, T.; Strozyk, M.; Castillo-Welter, F.; Drosdzol, C.; Haag, S. A New Reactor Concept for Conversion of CO$_2$ to Methanol. *Oil Gas-Eur. Mag.* **2021**, *47*, 28–32.

37. Girod, K.; Lohmann, H.; Schlüter, S.; Kaluza, S. Methanol Synthesis with Steel-Mill Gases: Simulation and Practical Testing of Selected Gas Utilization Scenarios. *Processes* **2020**, *8*, 1673. [CrossRef]

38. Girod, K.; Breitkreuz, K.; Hennig, T.; Lohmann, H.; Kaluza, S.; Schlüter, S. Steel Mills as Syngas Source for Methanol Synthesis: Simulation and Practical Performance Investigations. *Chem. Eng. Trans.* **2019**, *74*, 475–480.

39. Periodic Reporting for Period 3—FReSMe (From Residual Steel Gasses to Methanol) | H2020 | CORDIS | European Com-Mission. Available online: https://cordis.europa.eu/project/id/727504/reporting (accessed on 9 June 2022).

40. Lee, J.-K.; Lee, I.-B.; Han, J. Techno-economic analysis of methanol production from joint feedstock of coke oven gas and basic oxygen furnace gas from steel-making. *J. Ind. Eng. Chem.* **2019**, *75*, 77–85. [CrossRef]

41. Thonemann, N.; Maga, D. Life Cycle Assessment of Steel Mill Gas-Based Methanol Production within the Carbon2Chem®Project. *Chem. Ing. Tech.* **2020**, *92*, 1425–1430. [CrossRef]

42. Rigamonti, L.; Brivio, E. Life cycle assessment of methanol production by a carbon capture and utilization technology applied to steel mill gases. *Int. J. Greenh. Gas Control* **2022**, *115*, 103616. [CrossRef]

43. Müller, K.; Rachow, F.; Günther, V.; Schmeisser, D. Methanation of Coke Oven Gas with Nickel-Based Catalysts. *J. Environ. Sci.* **2019**, *4*, 73–79.

44. Razzaq, R.; Zhu, H.; Jiang, L.; Muhammad, U.; Li, C.; Zhang, S. Catalytic Methanation of CO and CO$_2$ in Coke Oven Gas over Ni–Co/ZrO$_2$–CeO$_2$. *Ind. Eng. Chem. Res.* **2013**, *52*, 2247–2256. [CrossRef]

45. Rosenfeld, D.C.; Böhm, H.; Lindorfer, J.; Lehner, M. Scenario analysis of implementing a power-to-gas and biomass gasification system in an integrated steel plant: A techno-economic and environmental study. *Renew. Energy* **2019**, *147*, 1511–1524. [CrossRef]

46. Perpiñán, J.; Bailera, M.; Romeo, L.M.; Peña, B.; Eveloy, V. CO$_2$ Recycling in the Iron and Steel Industry via Power-to-Gas and Oxy-Fuel Combustion. *Energies* **2021**, *14*, 7090. [CrossRef]

47. Wolf-Zoellner, P.; Medved, A.R.; Lehner, M.; Kieberger, N.; Rechberger, K. In Situ Catalytic Methanation of Real Steelworks Gases. *Energies* **2021**, *14*, 8131. [CrossRef]

48. Hauser, A.; Weitzer, M.; Gunsch, S.; Neubert, M.; Karl, J. Dynamic hydrogen-intensified methanation of synthetic by-product gases from steelworks. *Fuel Process. Technol.* **2021**, *217*, 106701. [CrossRef]

49. Zaccara, A.; Petrucciani, A.; Matino, I.; Branca, T.A.; Dettori, S.; Iannino, V.; Colla, V.; Bampaou, M.; Panopoulos, K. Renewable Hydrogen Production Processes for the Off-Gas Valorization in Integrated Steelworks through Hydrogen Intensified Methane and Methanol Syntheses. *Metals* **2020**, *10*, 1535. [CrossRef]

50. Bampaou, M.; Panopoulos, K.; Seferlis, P.; Voutetakis, S.; Matino, I.; Petrucciani, A.; Zaccara, A.; Colla, V.; Dettori, S.; Branca, T.A.; et al. Integration of Renewable Hydrogen Production in Steelworks Off-Gases for the Synthesis of Methanol and Methane. *Energies* **2021**, *14*, 2904. [CrossRef]

51. Kolb, S.; Plankenbühler, T.; Hofmann, K.; Bergerson, J.; Karl, J. Life cycle greenhouse gas emissions of renewable gas technologies: A comparative review. *Renew. Sustain. Energy Rev.* **2021**, *146*, 111147. [CrossRef]

52. Lee, J.H. Model predictive control: Review of the three decades of development. *Int. J. Control Autom. Syst.* **2011**, *9*, 415–424. [CrossRef]

53. Neubert, M.; Hauser, A.; Pourhossein, B.; Dillig, M.; Karl, J. Experimental evaluation of a heat pipe cooled structured reactor as part of a two-stage catalytic methanation process in power-to-gas applications. *Appl. Energy* **2018**, *229*, 289–298. [CrossRef]

54. Biegger, P.; Kirchbacher, F.; Medved, A.R.; Miltner, M.; Lehner, M.; Harasek, M. Development of Honeycomb Methanation Catalyst and Its Application in Power to Gas Systems. *Energies* **2018**, *11*, 1679. [CrossRef]

55. e Silva, D.P.; Salles, J.L.F.; Fardin, J.F.; Pereira, M.M.R. Management of an island and grid-connected microgrid using hybrid economic model predictive control with weather data. *Appl. Energy* **2020**, *278*, 115581. [CrossRef]

56. Dettori, S.; Matino, I.; Iannino, V.; Colla, V.; Hauser, A.; Wolf-Zöllner, P.; Haag, S. Optimizing methane and methanol production from integrated steelworks process off-gases through economic hybrid model predictive control. *IFAC-PapersOnLine* **2022**, *55*, 66–71. [CrossRef]

57. Bampaou, M.; Kyriakides, A.S.; Panopoulos, K.; Seferlis, P.; Voutetakis, S. Modelling of Methanol Synthesis: Improving Hydrogen Utilisation. *Chem. Eng. Trans.* **2021**, *88*, 931–936. [CrossRef]

58. Matino, I.; Dettori, S.; Colla, V.; Rechberger, K.; Kieberger, N. Echo-state neural networks forecasting steelworks off-gases for their dispatching in CH$_4$ and CH$_3$OH syntheses reactors. In Proceedings of the 29th European Symposium on Artificial Neural Networks, Computational Intelligence and Machine Learning, Online Conference, 6–8 October 2021. [CrossRef]

59. Matino, I.; Dettori, S.; Zaccara, A.; Petrucciani, A.; Iannino, V.; Colla, V.; Bampaou, M.; Panopoulos, K.; Rechberger, K.; Kolb, S.; et al. Hydrogen role in the valorization of integrated steelworks process off-gases through methane and methanol syntheses. *Matériaux Tech.* **2021**, *109*, 308. [CrossRef]

60. Medved, A.R.; Lehner, M.; Rosenfeld, D.C.; Lindorfer, J.; Rechberger, K. Enrichment of Integrated Steel Plant Process Gases with Implementation of Renewable Energy: Integration of Power-to-Gas and Biomass Gasification System in Steel Production. *Johns. Matthey Technol. Rev.* **2021**, *65*, 453–465. [CrossRef]